

### FEATURES

- Accurate rms-to-dc conversion from 50 Hz to 6 GHz
- Single-ended input dynamic range of >50 dB
- No balun or external input tuning required
- Waveform and modulation independent RF power detection
- Linear-in-decibels output, scaled: 52 mV/dB
- Log conformance error: <math>\pm 0.15\text{ dB}</math>
- Temperature stability: <math>\pm 0.5\text{ dB}</math>
- Voltage supply range: 4.5 V to 5.5 V
- Operating temperature range:  $-40^{\circ}\text{C}$  to  $+125^{\circ}\text{C}$
- Power-down capability to 1.5 mW
- Small footprint, 4 mm  $\times$  4 mm, LFCSP

### APPLICATIONS

- Power amplifier linearization/control loops
- Multi-Standard, Multi-Carrier Wireless Infrastructure  
(MCGSM, CDMA, WCDMA, TD-SCDMA, WiMAX, LTE)
- Transmitter power control
- Transmitter signal strength indication (TSSI)
- RF instrumentation

### GENERAL DESCRIPTION

The AD8363 is a true rms responding power detector that can be directly driven with a single-ended 50  $\Omega$  source. This feature makes the AD8363 frequency versatile by eliminating the need for a balun or any other form of external input tuning for operation up to 6 GHz.

The AD8363 provides an accurate power measurement, independent of waveform, for a variety of high frequency communication and instrumentation systems. Requiring only a single supply of 5 V and a few capacitors, it is easy to use and provides high measurement accuracy. The AD8363 can operate from arbitrarily low frequencies to 6 GHz and can accept inputs that have rms values from less than  $-50\text{ dBm}$  to at least  $0\text{ dBm}$ , with large crest factors exceeding the requirements for accurate measurement of WiMAX, CDMA, W-CDMA, TD-SCDMA, multicarrier GSM, and LTE signals.

The AD8363 can determine the true power of a high frequency signal having a complex low frequency modulation envelope, or it can be used as a simple low frequency rms voltmeter. The high-pass corner generated by its internal offset-nulling loop can be lowered by a capacitor added on the CHPF pin.

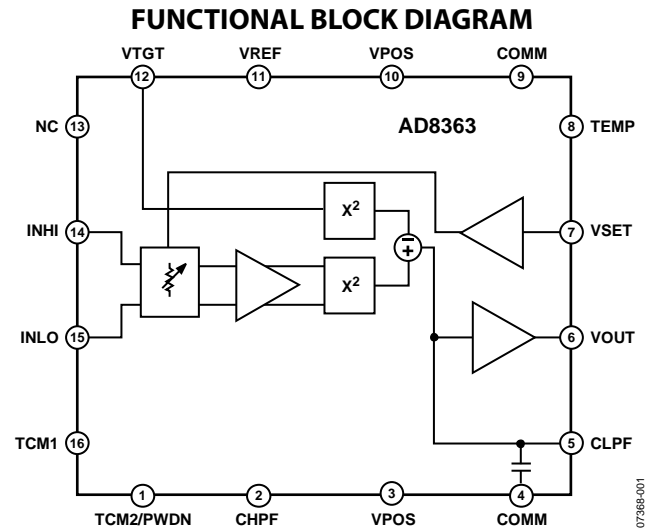


Figure 1. AD8363 Block Diagram

Used as a power measurement device, VOUT is connected to VSET. The output is then proportional to the logarithm of the rms value of the input. The reading is presented directly in decibels and is conveniently scaled to 52 mV/dB, or approximately 1 V per decade; however, other slopes are easily arranged. In controller mode, the voltage applied to VSET determines the power level required at the input to null the deviation from the setpoint. The output buffer can provide high load currents.

The AD8363 has 1.5 mW power consumption when powered down by a logic high applied to the TCM2/PWDN pin. It powers up within about 30  $\mu\text{s}$  to its nominal operating current of 60 mA at  $25^{\circ}\text{C}$ . The AD8363 is available in a 4 mm  $\times$  4 mm 16-lead LFCSP for operation over the  $-40^{\circ}\text{C}$  to  $+125^{\circ}\text{C}$  temperature range.

A fully populated RoHS compliant evaluation board is also available.

Rev. B

[Document Feedback](#)

Information furnished by Analog Devices is believed to be accurate and reliable. However, no responsibility is assumed by Analog Devices for its use, nor for any infringements of patents or other rights of third parties that may result from its use. Specifications subject to change without notice. No license is granted by implication or otherwise under any patent or patent rights of Analog Devices. Trademarks and registered trademarks are the property of their respective owners.

## TABLE OF CONTENTS

Features .....	1	VSET Interface.....	17
Applications.....	1	Output Interface .....	17
Functional Block Diagram .....	1	VTGT Interface .....	18
General Description .....	1	Measurement Mode Basic Connections.....	18
Revision History .....	2	System Calibration and Error Calculation.....	19
Specifications.....	3	Operation to 125°C.....	19
Absolute Maximum Ratings.....	7	Output Voltage Scaling.....	20
ESD Caution.....	7	Offset Compensation, Minimum $C_{LPF}$ , and Maximum $C_{HPF}$ Capacitance Values.....	20
Pin Configuration and Function Descriptions.....	8	Choosing a Value for $C_{LPF}$ .....	21
Typical Performance Characteristics .....	9	RF Pulse Response and VTGT .....	23
Theory of Operation .....	14	Controller Mode Basic Connections .....	23
Square Law Detector and Amplitude Target .....	14	Constant Output Power Operation.....	24
RF Input Interface .....	15	Description of RF Characterization.....	25
Choice of RF Input Pin .....	15	Evaluation and Characterization Circuit Board Layouts.....	26
Small Signal Loop Response .....	15	Assembly Drawings.....	28
Temperature Sensor Interface.....	16	Outline Dimensions .....	29
VREF Interface .....	16	Ordering Guide .....	29
Temperature Compensation Interface.....	16		
Power-Down Interface.....	17		

## REVISION HISTORY

### 3/15—Rev. A to Rev. B

Changes to Figure 2 and Table 3.....	8
Changes to Controller Mode Basic Connections Section.....	23
Updated Outline Dimensions.....	29
Changes to the Ordering Guide.....	29

### 7/11—Rev. 0 to Rev. A

Changes to Features Section and Applications Section.....	1
Added 3-Point Calibration to Table 1 for All MHz.....	3
Replaced Typical Performance Characteristics Section; Renumbered Sequentially.....	9
Changes to Theory of Operation Section.....	14
Changes to Temperature Compensation Interface Section .....	16
Changes to System Calibration and Error Calculation Section and Changes to Figure 44 and Figure 45 .....	19
Deleted Basis for Error Calculations Section.....	20
Changes to Figure 46.....	20
Deleted Selecting and Increasing Calibration Points to Improve Accuracy over a Reduced Range Section.....	22
Deleted Altering the Slope Section .....	23
Added Output Voltage Scaling Section .....	23

### 5/09—Revision 0: Initial Version

## SPECIFICATIONS

$V_{POS} = 5\text{ V}$ ,  $T_A = 25^\circ\text{C}$ ,  $Z_O = 50\ \Omega$ , single-ended input drive,  $V_{OUT}$  connected to  $V_{SET}$ ,  $V_{TGT} = 1.4\text{ V}$ ,  $C_{LPF} = 3.9\text{ nF}$ ,  $C_{HPF} = 2.7\text{ nF}$ , error referred to best-fit line (linear regression) from  $-20\text{ dBm}$  to  $-40\text{ dBm}$ , unless otherwise noted.

Table 1.

Parameter	Conditions	Min	Typ	Max	Unit
<b>OVERALL FUNCTION</b>					
Maximum Input Frequency				6	GHz
<b>RF INPUT INTERFACE</b>					
Input Resistance	INHI (Pin 14), INLO (Pin 15), ac-coupled Single-ended drive		50		$\Omega$
Common-Mode DC Voltage			2.6		V
<b>100 MHz</b>					
Output Voltage: High Power In	TCM1 (Pin 16) = 0.47 V, TCM2 (Pin 1) = 1.0 V, INHI input $P_{IN} = -10\text{ dBm}$		2.47		V
Output Voltage: Low Power In	$P_{IN} = -40\text{ dBm}$		0.92		V
$\pm 1.0\text{ dB}$ Dynamic Range	CW input, $T_A = 25^\circ\text{C}$ 3-point calibration at 0 dBm, $-10\text{ dBm}$ , and $-40\text{ dBm}$ Best-fit (linear regression) at $-20\text{ dBm}$ and $-40\text{ dBm}$		64		dB
Maximum Input Level, $\pm 1.0\text{ dB}$			65		dB
Minimum Input Level, $\pm 1.0\text{ dB}$			9		dBm
Deviation vs. Temperature	Deviation from output at $25^\circ\text{C}$ $-40^\circ\text{C} < T_A < +85^\circ\text{C}$ ; $P_{IN} = -10\text{ dBm}$ $-40^\circ\text{C} < T_A < +85^\circ\text{C}$ ; $P_{IN} = -40\text{ dBm}$		$-0.2/+0.3$ $-0.5/+0.6$		dB
Logarithmic Slope			51.7		mV/dB
Logarithmic Intercept			$-58$		dBm
Deviation from CW Response	13 dB peak-to-rms ratio (W-CDMA), over 40 dB dynamic range 12 dB peak-to-rms ratio (WiMAX), over 40 dB dynamic range 14.0 dB peak-to-rms ratio (16C CDMA2K), over 40 dB dynamic range 256 QAM, CF = 8 dB, over 40 dB dynamic range		$<\pm 0.1$ $<\pm 0.1$ $<\pm 0.1$ $<\pm 0.1$		dB
Input Impedance	Single-ended drive		$49 - j0.09$		$\Omega$
<b>900 MHz</b>					
Output Voltage: High Power In	TCM1 (Pin 16) = 0.5 V, TCM2 (Pin 1) = 1.2 V, INHI input $P_{IN} = -15\text{ dBm}$		2.2		V
Output Voltage: Low Power In	$P_{IN} = -40\text{ dBm}$		0.91		V
$\pm 1.0\text{ dB}$ Dynamic Range	CW input, $T_A = 25^\circ\text{C}$ 3-point calibration at 0 dBm, $-10\text{ dBm}$ , and $-40\text{ dBm}$ Best-fit (linear regression) at $-20\text{ dBm}$ and $-40\text{ dBm}$		60		dB
Maximum Input Level, $\pm 1.0\text{ dB}$			54		dB
Minimum Input Level, $\pm 1.0\text{ dB}$			$-2$		dBm
Deviation vs. Temperature	Deviation from output at $25^\circ\text{C}$ $-40^\circ\text{C} < T_A < +85^\circ\text{C}$ ; $P_{IN} = -15\text{ dBm}$ $-40^\circ\text{C} < T_A < +85^\circ\text{C}$ ; $P_{IN} = -40\text{ dBm}$		$+0.6/-0.4$ $+0.8/-0.6$		dB
Logarithmic Slope			51.8		mV/dB
Logarithmic Intercept			$-58$		dBm
Deviation from CW Response	13 dB peak-to-rms ratio (W-CDMA), over 40 dB dynamic range 12 dB peak-to-rms ratio (WiMAX), over 40 dB dynamic range 14.0 dB peak-to-rms ratio (16C CDMA2K), over 40 dB dynamic range 256 QAM, CF = 8 dB, over 40 dB dynamic range		$<\pm 0.1$ $<\pm 0.1$ $<\pm 0.1$ $<\pm 0.1$		dB
Input Impedance	Single-ended drive		$60 - j3.3$		$\Omega$

Parameter	Conditions	Min	Typ	Max	Unit
1.9 GHz	TCM1 (Pin 16) = 0.52 V, TCM2 (Pin 1) = 0.51 V, INHI input				
Output Voltage: High Power In	$P_{IN} = -15$ dBm		2.10		V
Output Voltage: Low Power In	$P_{IN} = -40$ dBm		0.8		V
$\pm 1.0$ dB Dynamic Range	CW input, $T_A = 25^\circ\text{C}$ 3-point calibration at 0 dBm, $-10$ dBm, and $-40$ dBm Best-fit (linear regression) at $-20$ dBm and $-40$ dBm		56		dB
Maximum Input Level, $\pm 1.0$ dB			48		dB
Minimum Input Level, $\pm 1.0$ dB			$-6$		dBm
Deviation vs. Temperature	Deviation from output at $25^\circ\text{C}$ $-40^\circ\text{C} < T_A < +85^\circ\text{C}$ ; $P_{IN} = -15$ dBm $-40^\circ\text{C} < T_A < +85^\circ\text{C}$ ; $P_{IN} = -40$ dBm		$+0.3/-0.5$		dB
Logarithmic Slope			$+0.4/-0.4$		dB
Logarithmic Intercept			52		mV/dB
Deviation from CW Response	13 dB peak-to-rms ratio (W-CDMA), over 37 dB dynamic range 12 dB peak-to-rms ratio (WiMAX), over 37 dB dynamic range 14.0 dB peak-to-rms ratio (16C CDMA2K), over 37 dB dynamic range		$\pm 0.1$		dB
	256 QAM, CF = 8 dB, over 37 dB dynamic range		$\pm 0.1$		dB
Input Impedance	Single-ended drive		$118 - j26$		$\Omega$
2.14 GHz	TCM1 (Pin 16) = 0.52 V, TCM2 (Pin 1) = 0.6 V, INHI input				
Output Voltage: High Power In	$P_{IN} = -15$ dBm		2.0		V
Output Voltage: Low Power In	$P_{IN} = -40$ dBm		0.71		V
$\pm 1.0$ dB Dynamic Range	CW input, $T_A = 25^\circ\text{C}$ 3-point calibration at 0 dBm, $-10$ dBm and $-40$ dBm Best-fit (linear regression) at $-20$ dBm and $-40$ dBm		55		dB
Maximum Input Level, $\pm 1.0$ dB			44		dB
Minimum Input Level, $\pm 1.0$ dB			$-8$		dBm
Deviation vs. Temperature	Deviation from output at $25^\circ\text{C}$ $-40^\circ\text{C} < T_A < +85^\circ\text{C}$ ; $P_{IN} = -15$ dBm $-40^\circ\text{C} < T_A < +85^\circ\text{C}$ ; $P_{IN} = -40$ dBm		$+0.1/-0.2$		dB
Logarithmic Slope			$+0.3/-0.5$		dB
Logarithmic Intercept			52.2		mV/dB
Deviation from CW Response	13 dB peak-to-rms ratio (W-CDMA), over 35 dB dynamic range 12 dB peak-to-rms ratio (WiMAX), over 35 dB dynamic range 14.0 dB peak-to-rms ratio (16C CDMA2K), over 35 dB dynamic range		$\pm 0.1$		dB
	256 QAM, CF = 8 dB, over 35 dB dynamic range		$\pm 0.1$		dB
Rise Time	Transition from no input to 1 dB settling at $RF_{IN} = -10$ dBm, $C_{LPF} = 390$ pF, $C_{HPF} = \text{open}$		3		$\mu\text{s}$
Fall Time	Transition from $-10$ dBm to within 1 dB of final value (that is, no input level), $C_{LPF} = 390$ pF, $C_{HPF} = \text{open}$		15		$\mu\text{s}$
Input Impedance	Single-ended drive		$130 - j49$		$\Omega$
2.6 GHz	TCM1 (Pin 16) = 0.54 V, TCM2 (Pin 1) = 1.1 V, INHI input				
Output Voltage: High Power In	$P_{IN} = -15$ dBm		1.84		V
Output Voltage: Low Power In	$P_{IN} = -40$ dBm		0.50		V
$\pm 1.0$ dB Dynamic Range	CW input, $T_A = 25^\circ\text{C}$ 3-point calibration at 0 dBm, $-10$ dBm and $-40$ dBm Best-fit (linear regression) at $-20$ dBm and $-40$ dBm		50		dB
Maximum Input Level, $\pm 1.0$ dB			41		dB
Minimum Input Level, $\pm 1.0$ dB			$-7$		dBm
Deviation vs. Temperature	Deviation from output at $25^\circ\text{C}$ $-40^\circ\text{C} < T_A < +85^\circ\text{C}$ ; $P_{IN} = -15$ dBm $-40^\circ\text{C} < T_A < +85^\circ\text{C}$ ; $P_{IN} = -40$ dBm		$+0.5/-0.2$		dB
			$+0.6/-0.2$		dB

Parameter	Conditions	Min	Typ	Max	Unit
Logarithmic Slope			52.9		mV/dB
Logarithmic Intercept			-49		dBm
Deviation from CW Response	13 dB peak-to-rms ratio (W-CDMA), over 32 dB dynamic range		±0.1		dB
	12 dB peak-to-rms ratio (WiMAX), over 32 dB dynamic range		±0.1		dB
	14.0 dB peak-to-rms ratio (16C CDMA2K), over 32 dB dynamic range		±0.1		dB
Input Impedance	256 QAM, CF = 8 dB, over 32 dB dynamic range		±0.1		dB
	Single-ended drive		95 - j65		Ω
3.8 GHz	TCM1 (Pin 16) = 0.56 V, TCM2 (Pin 1) = 1.0 V, INLO input				
Output Voltage: High Power In	P <sub>IN</sub> = -20 dBm		1.54		V
Output Voltage: Low Power In	P <sub>IN</sub> = -40 dBm		0.54		V
±1.0 dB Dynamic Range	CW input, T <sub>A</sub> = 25°C				
	3-point calibration at 0 dBm, -10 dBm and -40 dBm		50		dB
	Best-fit (linear regression) at -20 dBm and -40 dBm		43		dB
Maximum Input Level, ±1.0 dB			-5		dBm
Minimum Input Level, ±1.0 dB			-48		dBm
Deviation vs. Temperature	Deviation from output at 25°C				
	-40°C < T <sub>A</sub> < +85°C; P <sub>IN</sub> = -20 dBm		+0.1/-0.7		dB
	-40°C < T <sub>A</sub> < +85°C; P <sub>IN</sub> = -40 dBm		+0.4/-0.5		dB
Logarithmic Slope			50.0		mV/dB
Logarithmic Intercept			-51		dBm
Deviation from CW Response	13 dB peak-to-rms ratio (W-CDMA), over 32 dB dynamic range		±0.1		dB
	12 dB peak-to-rms ratio (WiMAX), over 32 dB dynamic range		±0.1		dB
	14.0 dB peak-to-rms ratio (16C CDMA2K), over 32 dB dynamic range		±0.1		dB
Input Impedance	256 QAM, CF = 8 dB, over 32 dB dynamic range		±0.1		dB
	Single-ended drive		42 - j4.5		Ω
5.8 GHz	TCM1 (Pin 16) = 0.88 V, TCM2 (Pin 1) = 1.0 V, INLO input				
Output Voltage: High Power In	P <sub>IN</sub> = -20 dBm		1.38		V
Output Voltage: Low Power In	P <sub>IN</sub> = -40 dBm		0.36		V
±1.0 dB Dynamic Range	CW input, T <sub>A</sub> = 25°C				
	3-point calibration at 0 dBm, -10 dBm and -40 dBm		50		dB
	Best-fit (linear regression) at -20 dBm and -40 dBm		45		dB
Maximum Input Level, ±1.0 dB			-3		dBm
Minimum Input Level, ±1.0 dB			-48		dBm
Deviation vs. Temperature	Deviation from output at 25°C				
	-40°C < T <sub>A</sub> < +85°C; P <sub>IN</sub> = -20 dBm		+0.1/-0.6		dB
	-40°C < T <sub>A</sub> < +85°C; P <sub>IN</sub> = -40 dBm		+0.3/-0.8		dB
Logarithmic Slope			51.1		mV/dB
Logarithmic Intercept			-47		dBm
Deviation from CW Response	13 dB peak-to-rms ratio (W-CDMA), over 32 dB dynamic range		±0.1		dB
	12 dB peak-to-rms ratio (WiMAX), over 32 dB dynamic range		±0.1		dB
	14.0 dB peak-to-rms ratio (16C CDMA2K), over 32 dB dynamic range		±0.1		dB
Input Impedance	256 QAM, CF = 8 dB, over 32 dB dynamic range		±0.1		dB
	Single-ended drive		28 + j1.6		Ω
OUTPUT INTERFACE	VOUT (Pin 6)				
Output Swing, Controller Mode	Swing range minimum, R <sub>L</sub> ≥ 500 Ω to ground		0.03		V
	Swing range maximum, R <sub>L</sub> ≥ 500 Ω to ground		4.8		V
Current Source/Sink Capability	Output held at V <sub>POS</sub> /2			10/10	mA
Voltage Regulation	I <sub>LOAD</sub> = 8 mA, source/sink		-0.2/+0.1		%
Rise Time	Transition from no input to 1 dB settling at R <sub>F IN</sub> = -10 dBm, C <sub>LPF</sub> = 390 pF, C <sub>HPF</sub> = open		3		μs

Parameter	Conditions	Min	Typ	Max	Unit
Fall Time	Transition from $-10$ dBm to within 1 dB of final value (that is, no input level), $C_{LPF} = 390$ pF, $C_{HPF} =$ open		15		$\mu$ s
Noise Spectral Density	Measured at 100 kHz		45		nV/ $\sqrt$ Hz
SETPOINT INPUT	VSET (Pin 7)				
Voltage Range	Log conformance error $\leq 1$ dB, minimum 2.14 GHz Log conformance error $\leq 1$ dB, maximum 2.14 GHz		2.0 0.7		V V
Input Resistance			72		k $\Omega$
Logarithmic Scale Factor	$f = 2.14$ GHz, $-40^{\circ}\text{C} \leq T_A \leq +85^{\circ}\text{C}$		19.2		dB/V
Logarithmic Intercept	$f = 2.14$ GHz, $-40^{\circ}\text{C} \leq T_A \leq +85^{\circ}\text{C}$ , referred to 50 $\Omega$		-54		dBm
TEMPERATURE COMPENSATION	TCM1 (Pin 16), TCM2 (Pin 1)				
Input Voltage Range		0		2.5	V
Input Bias Current, TCM1	$V_{TCM1} = 0$ V $V_{TCM1} = 0.5$ V		-140 80		$\mu$ A $\mu$ A
Input Resistance, TCM1	$V_{TCM1} > 0.7$ V		5		k $\Omega$
Input Current, TCM2	$V_{TCM2} = 5$ V $V_{TCM2} = 4.5$ V $V_{TCM2} = 1$ V $V_{TCM2} = 0$ V		2 750 -2 -3		$\mu$ A $\mu$ A $\mu$ A $\mu$ A
Input Resistance, TCM2	$0.7$ V $\leq V_{TCM2} \leq 4.0$ V		500		k $\Omega$
VOLTAGE REFERENCE	VREF (Pin 11)				
Output Voltage	$RF_{IN} = -55$ dBm		2.3		V
Temperature Sensitivity	$25^{\circ}\text{C} \leq T_A \leq 70^{\circ}\text{C}$ $70^{\circ}\text{C} \leq T_A \leq 125^{\circ}\text{C}$ $-40^{\circ}\text{C} \leq T_A \leq +25^{\circ}\text{C}$		0.04 -0.06 -0.18		mV/ $^{\circ}$ C mV/ $^{\circ}$ C mV/ $^{\circ}$ C
Current Source/Sink Capability	$25^{\circ}\text{C} \leq T_A \leq 125^{\circ}\text{C}$ $-40^{\circ}\text{C} \leq T_A < +25^{\circ}\text{C}$			4/0.05 3/0.05	mA mA
Voltage Regulation	$T_A = 25^{\circ}\text{C}$ , $I_{LOAD} = 3$ mA		-0.6		%
TEMPERATURE REFERENCE	TEMP (Pin 8)				
Output Voltage	$T_A = 25^{\circ}\text{C}$ , $R_L \geq 10$ k $\Omega$		1.4		V
Temperature Coefficient	$-40^{\circ}\text{C} \leq T_A \leq +125^{\circ}\text{C}$ , $R_L \geq 10$ k $\Omega$		5		mV/ $^{\circ}$ C
Current Source/Sink Capability	$25^{\circ}\text{C} \leq T_A \leq 125^{\circ}\text{C}$ $-40^{\circ}\text{C} \leq T_A < +25^{\circ}\text{C}$			4/0.05 3/0.05	mA mA
Voltage Regulation	$T_A = 25^{\circ}\text{C}$ , $I_{LOAD} = 3$ mA		-0.1		%
RMS TARGET INTERFACE	VTGT (Pin 12)				
Input Voltage Range		1.4		2.5	V
Input Bias Current	$V_{TGT} = 1.4$ V		14		$\mu$ A
Input Resistance			100		k $\Omega$
POWER-DOWN INTERFACE	TCM2 (Pin 1)				
Logic Level to Enable	VPWDN decreasing		4.2		V
Logic Level to Disable	VPWDN increasing		4.7		V
Input Current	$V_{TCM2} = 5$ V $V_{TCM2} = 4.5$ V $V_{TCM2} = 1$ V $V_{TCM2} = 0$ V		2 750 -2 -3		$\mu$ A $\mu$ A $\mu$ A $\mu$ A
Enable Time	TCM2 low to $V_{OUT}$ at 1 dB of final value, $C_{LPF} = 470$ pF, $C_{HPF} = 220$ pF, $RF_{IN} = 0$ dBm		35		$\mu$ s
Disable Time	TCM2 high to $V_{OUT}$ at 1 dB of final value, $C_{LPF} = 470$ pF, $C_{HPF} = 220$ pF, $RF_{IN} = 0$ dBm		25		$\mu$ s
POWER SUPPLY INTERFACE	VPOS (Pin 3, Pin 10)				
Supply Voltage		4.5	5	5.5	V
Quiescent Current	$T_A = 25^{\circ}\text{C}$ , $RF_{IN} = -55$ dBm $T_A = 85^{\circ}\text{C}$		60 72		mA mA
Power-Down Current	$V_{TCM2} > V_{POS} - 0.3$ V		300		$\mu$ A

## ABSOLUTE MAXIMUM RATINGS

Table 2.

Parameter	Rating
Supply Voltage, VPOS	5.5 V
Input Average RF Power <sup>1</sup>	21 dBm
Equivalent Voltage, Sine Wave Input	2.51 V rms
Internal Power Dissipation	450 mW
$\theta_{JC}^2$	10.6°C/W
$\theta_{JB}^2$	35.3°C/W
$\theta_{JA}^2$	57.2°C/W
$\Psi_{JT}^2$	1.0°C/W
$\Psi_{JB}^2$	34°C/W
Maximum Junction Temperature	150°C
Operating Temperature Range	−40°C to +125°C
Storage Temperature Range	−65°C to +150°C
Lead Temperature (Soldering, 60 sec)	300°C

<sup>1</sup> This is for long durations. Excursions above this level, with durations much less than 1 second, are possible without damage.

<sup>2</sup> No airflow with the exposed pad soldered to a 4-layer JEDEC board.

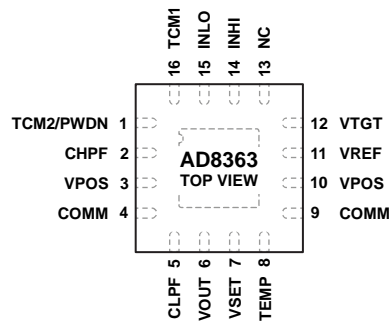
Stresses at or above those listed under Absolute Maximum Ratings may cause permanent damage to the product. This is a stress rating only; functional operation of the product at these or any other conditions above those indicated in the operational section of this specification is not implied. Operation beyond the maximum operating conditions for extended periods may affect product reliability.

### ESD CAUTION



**ESD (electrostatic discharge) sensitive device.** Charged devices and circuit boards can discharge without detection. Although this product features patented or proprietary protection circuitry, damage may occur on devices subjected to high energy ESD. Therefore, proper ESD precautions should be taken to avoid performance degradation or loss of functionality.

## PIN CONFIGURATION AND FUNCTION DESCRIPTIONS



## NOTES

1. NC = NO CONNECT. DO NOT CONNECT TO THIS PIN.
2. THE EXPOSED PAD IS THE SYSTEM COMMON CONNECTION AND IT MUST HAVE BOTH A GOOD THERMAL AND GOOD ELECTRICAL CONNECTION TO GROUND.

077866-002

Figure 2. Pin Configuration

Table 3. Pin Function Descriptions

Pin No.	Mnemonic	Description	Equivalent Circuit
1	TCM2/PWDN	This is a dual function pin used for controlling the amount of nonlinear intercept temperature compensation at voltages <2.5 V and/or for shutting down the device at voltages >4 V. If the shutdown function is not used, this pin can be connected to the VREF pin through a voltage divider.	See Figure 39
2	CHPF	Connect this pin to VPOS via a capacitor to determine the –3 dB point of the input signal high-pass filter. Only add a capacitor when operating at frequencies below 10 MHz.	See Figure 48
3, 10	VPOS	Supply for the Device. Connect these pins to a 5 V power supply. Pin 3 and Pin 10 are not internally connected; therefore, both must connect to the source.	Not applicable
4, 9	COMM	System Common Connection. Connect these pins via low impedance to system common.	Not applicable
5	CLPF	Connection for Loop Filter Integration (Averaging) Capacitor. Connect a ground-referenced capacitor to this pin. A resistor can be connected in series with this capacitor to improve loop stability and response time. Minimum $C_{LPF}$ value is 390 pF.	See Figure 41
6	VOUT	Output Pin in Measurement Mode (Error Amplifier Output). In measurement mode, this pin is connected to VSET. This pin can be used to drive a gain control when the device is used in controller mode.	See Figure 41
7	VSET	The voltage applied to this pin sets the decibel value of the required RF input voltage that results in zero current flow in the loop integrating capacitor pin, CLPF. This pin controls the variable gain amplifier (VGA) gain such that a 50 mV change in VSET reduces the gain by approximately 1 dB.	See Figure 40
8	TEMP	Temperature Sensor Output.	See Figure 35
11	VREF	General-Purpose Reference Voltage Output of 2.3 V.	See Figure 36
12	VTGT	The voltage applied to this pin determines the target power at the input of the RF squaring circuit. The intercept voltage is proportional to the voltage applied to this pin. The use of a lower target voltage increases the crest factor capacity; however, this may affect the system loop response.	See Figure 42
13	NC	No Connect.	Not applicable
14	INHI	This is the RF input pin for frequencies up to and including 2.6 GHz. The RF input signal is normally ac-coupled to this pin through a coupling capacitor.	See Figure 34
15	INLO	This is the RF input pin for frequencies above 2.6 GHz. The RF input signal is normally ac-coupled to this pin through a coupling capacitor.	See Figure 34
16	TCM1	This pin is used to adjust the intercept temperature compensation. Connect this pin to VREF through a voltage divider or to an external dc source.	See Figure 38
	EPAD	Exposed Pad. The exposed pad is the system common connection and it must have both a good thermal and good electrical connection to ground.	Not applicable



### TYPICAL PERFORMANCE CHARACTERISTICS

$V_{POS} = 5\text{ V}$ ,  $Z_O = 50\ \Omega$ , single-ended input drive,  $V_{OUT}$  connected to  $V_{SET}$ ,  $V_{TGT} = 1.4\text{ V}$ ,  $C_{LPF} = 3.9\text{ nF}$ ,  $C_{HPF} = 2.7\text{ nF}$ ,  $T_A = +25^\circ\text{C}$  (black),  $-40^\circ\text{C}$  (blue),  $+85^\circ\text{C}$  (red), where appropriate. Error calculated using 3-point calibration at 0 dBm,  $-10\text{ dBm}$ , and  $-40\text{ dBm}$ , unless otherwise indicated. Input RF signal is a sine wave (CW), unless otherwise indicated.

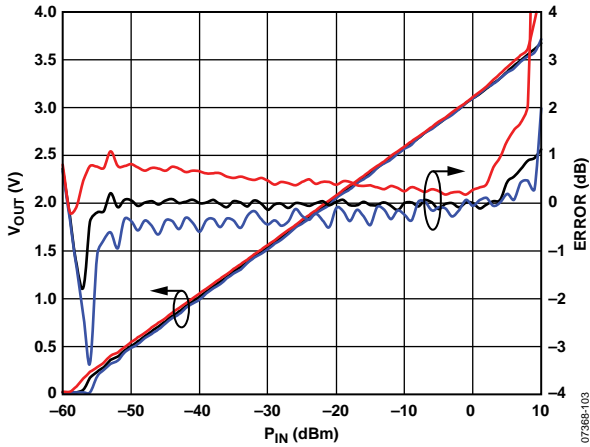


Figure 3.  $V_{OUT}$  and Log Conformance vs. Input Power and Temperature at 100 MHz

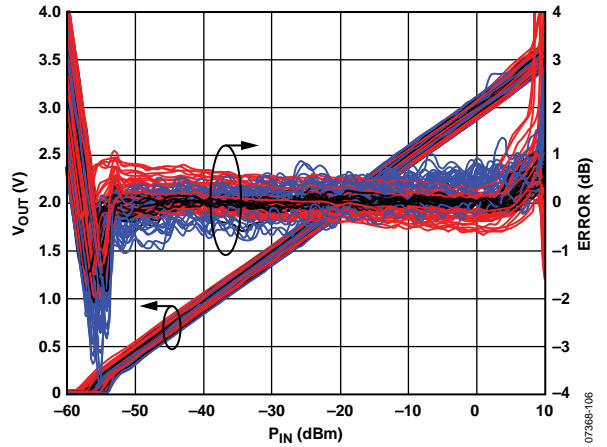


Figure 6. Distribution of  $V_{OUT}$  and Error with Respect to  $25^\circ\text{C}$  Ideal Line over Temperature vs. Input Amplitude at 100 MHz, CW

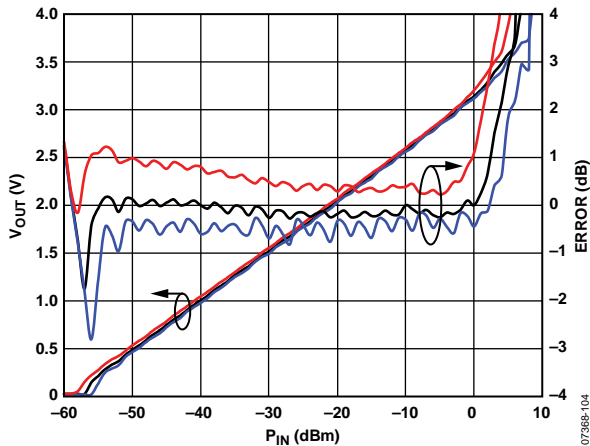


Figure 4.  $V_{OUT}$  and Log Conformance Error with Respect to  $25^\circ\text{C}$  Ideal Line over Temperature vs. Input Amplitude at 900 MHz, CW, Typical Device

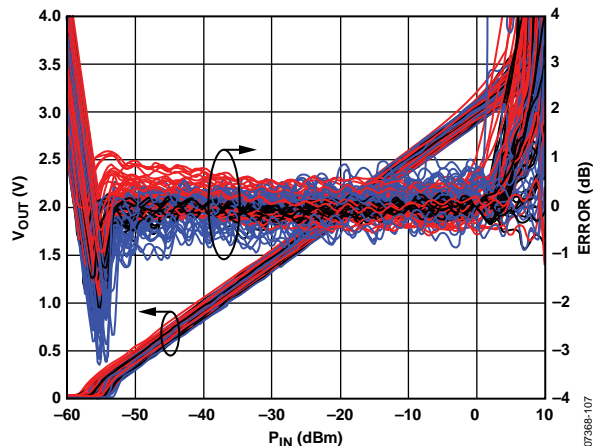


Figure 7. Distribution of  $V_{OUT}$  and Error with Respect to  $25^\circ\text{C}$  Ideal Line over Temperature vs. Input Amplitude at 900 MHz, CW

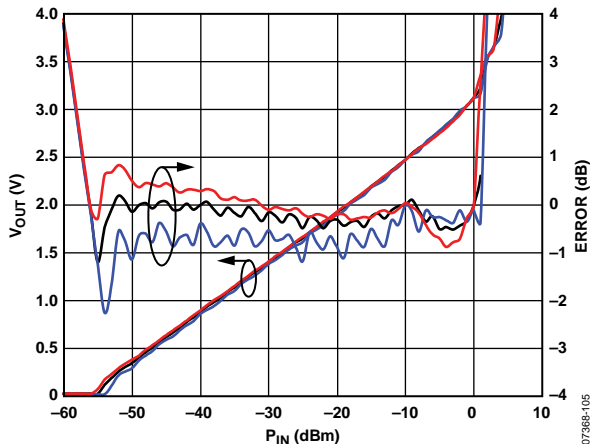


Figure 5.  $V_{OUT}$  and Log Conformance Error with Respect to  $25^\circ\text{C}$  Ideal Line over Temperature vs. Input Amplitude at 1.90 GHz, CW, Typical Device

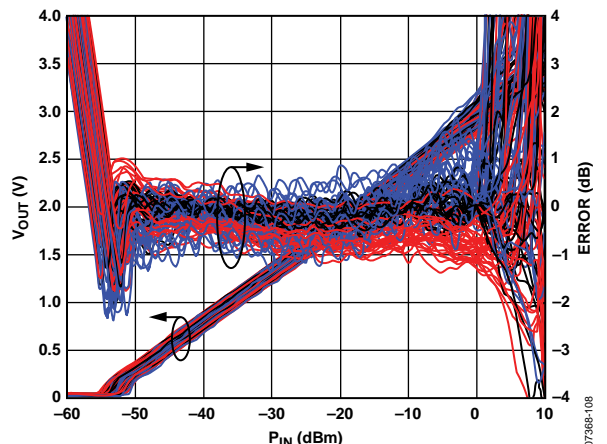


Figure 8. Distribution of  $V_{OUT}$  and Error with Respect to  $25^\circ\text{C}$  Ideal Line over Temperature vs. Input Amplitude at 1.90 GHz, CW

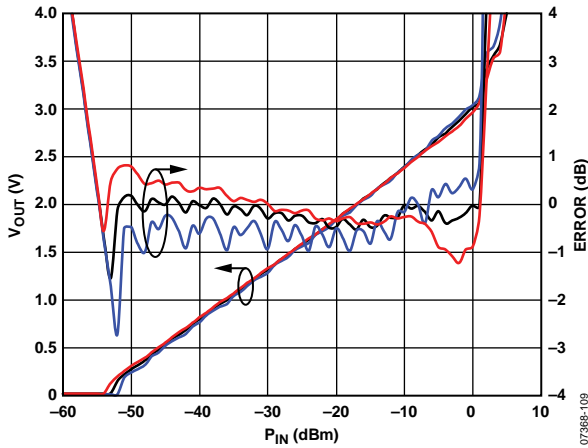


Figure 9.  $V_{OUT}$  and Log Conformance Error with Respect to 25°C Ideal Line over Temperature vs. Input Amplitude at 2.14 GHz, CW, Typical Device

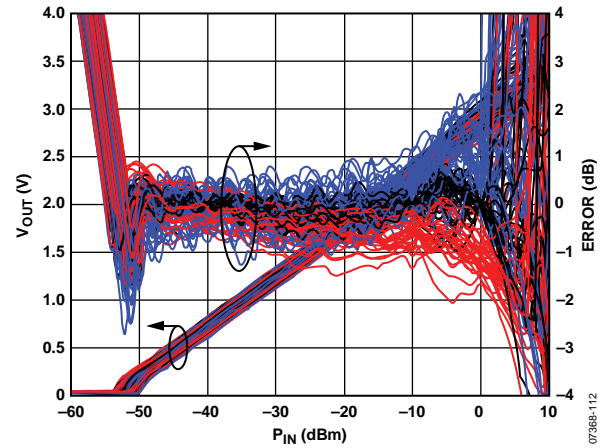


Figure 12. Distribution of  $V_{OUT}$  and Error with Respect to 25°C Ideal Line over Temperature vs. Input Amplitude at 2.14 GHz, CW

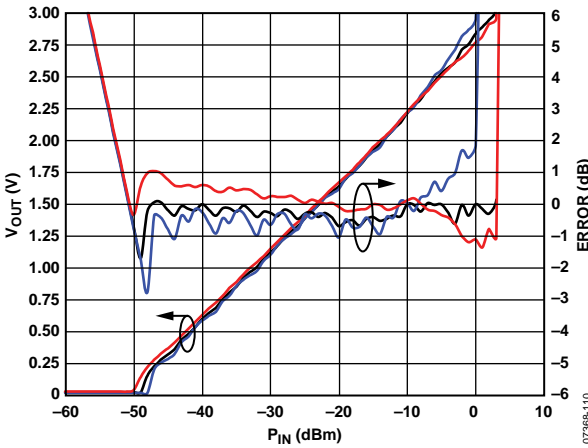


Figure 10.  $V_{OUT}$  and Log Conformance Error with Respect to 25°C Ideal Line over Temperature vs. Input Amplitude at 2.6 GHz, CW, Typical Device

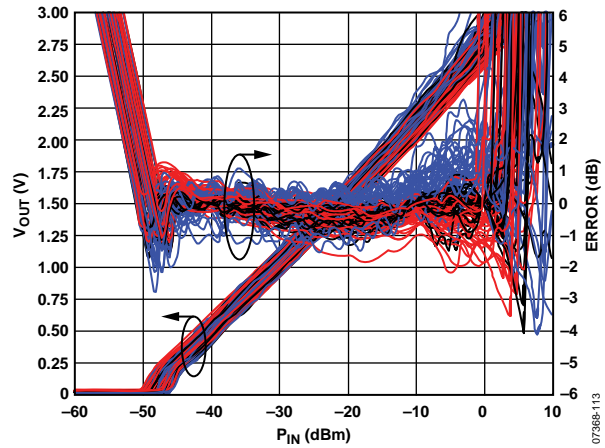


Figure 13. Distribution of  $V_{OUT}$  and Error with Respect to 25°C Ideal Line over Temperature vs. Input Amplitude at 2.6 GHz, CW

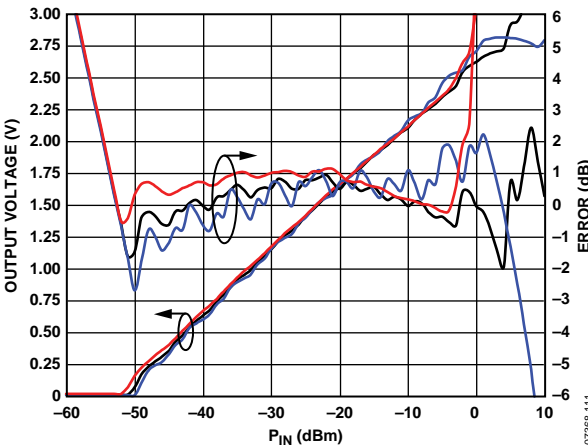


Figure 11.  $V_{OUT}$  and Log Conformance Error with Respect to 25°C Ideal Line over Temperature vs. Input Amplitude at 3.8 GHz, CW, Typical Device

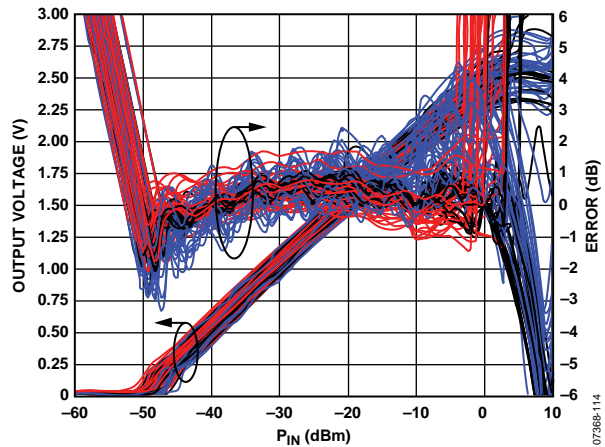


Figure 14. Distribution of  $V_{OUT}$  and Error with Respect to 25°C Ideal Line over Temperature vs. Input Amplitude at 3.8 GHz, CW

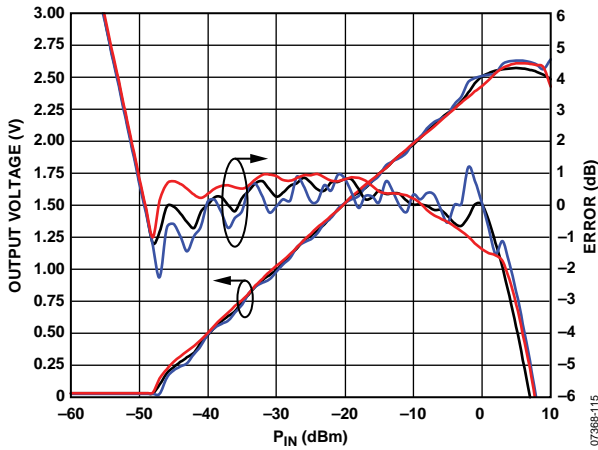


Figure 15.  $V_{OUT}$  and Log Conformance Error with Respect to 25°C Ideal Line over Temperature vs. Input Amplitude at 5.8 GHz, Typical Device

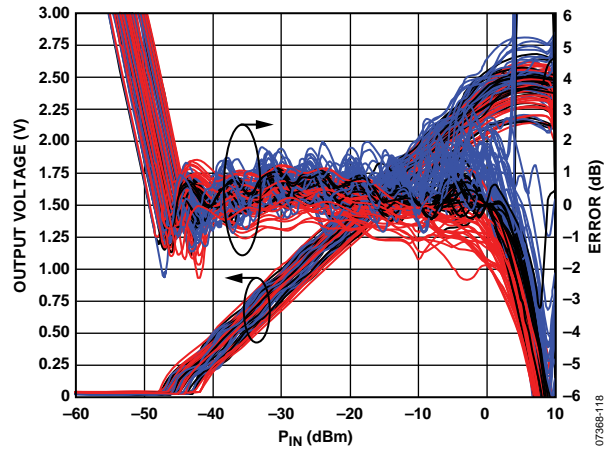


Figure 18. Distribution of  $V_{OUT}$  and Error with Respect to 25°C Ideal Line over Temperature vs. Input Amplitude at 5.8 GHz, CW

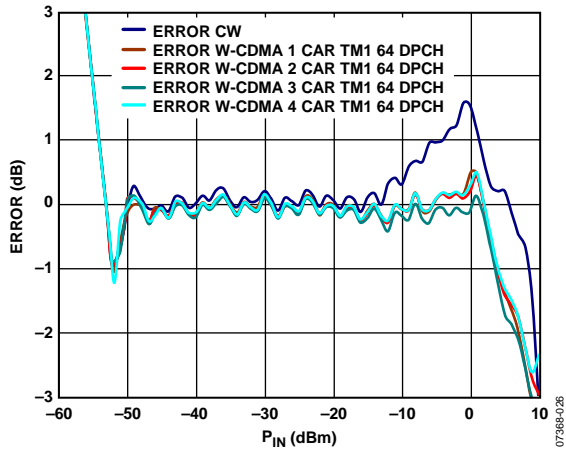


Figure 16. Error from CW Linear Reference vs. Input Amplitude with Modulation, Frequency at 2.14 GHz,  $C_{LPF} = 0.1 \mu F$ , INHI Input

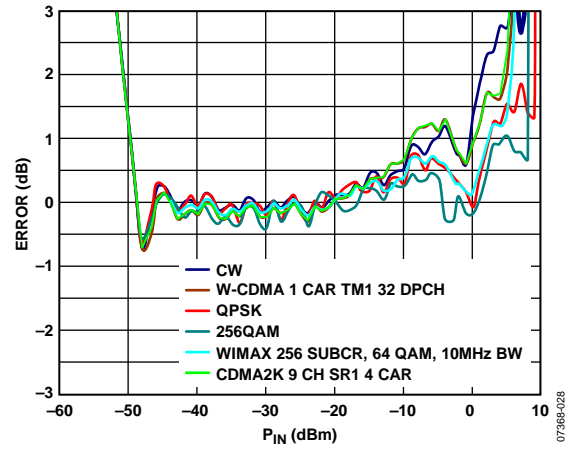


Figure 19. Error from CW Linear Reference vs. Input Amplitude with Modulation, Frequency at 2.6 GHz,  $C_{LPF} = 0.1 \mu F$ , INHI Input

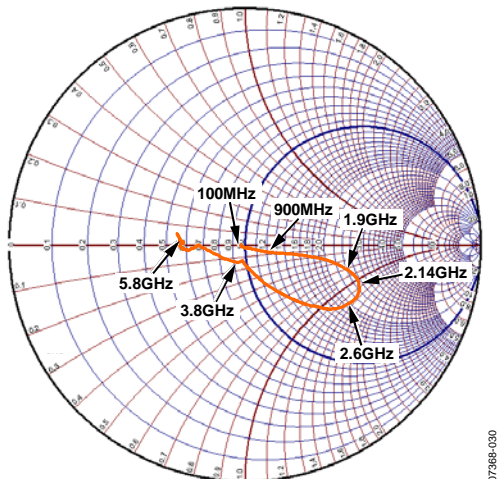


Figure 17. Single-Ended Input Impedance ( $S_{11}$ ) vs. Frequency;  $Z_0 = 50 \Omega$ , INHI or INLO

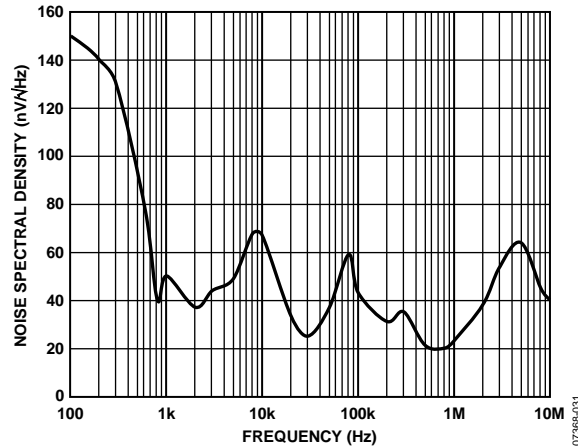


Figure 20. Typical Noise Spectral Density of  $V_{OUT}$ ; All  $C_{LPF}$  Values

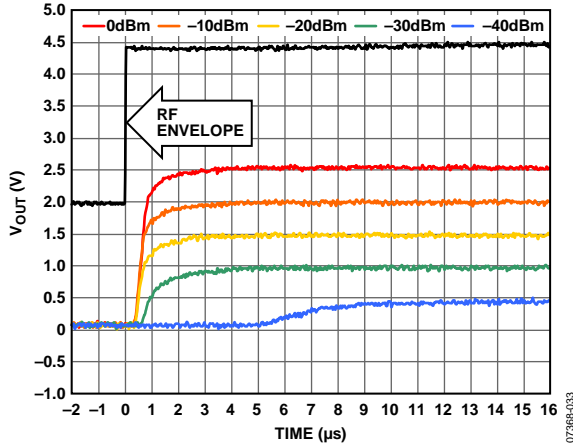


Figure 21. Output Response to RF Burst Input, Carrier Frequency at 2.14 GHz,  $C_{LPF} = 390\text{ pF}$ ,  $C_{HPF} = \text{Open}$ , Rising Edge

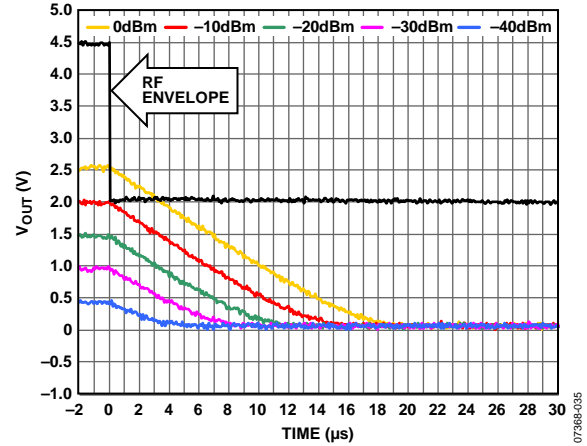


Figure 24. Output Response to RF Burst Input, Carrier Frequency at 2.14 GHz,  $C_{LPF} = 390\text{ pF}$ ,  $C_{HPF} = \text{Open}$ , Falling Edge

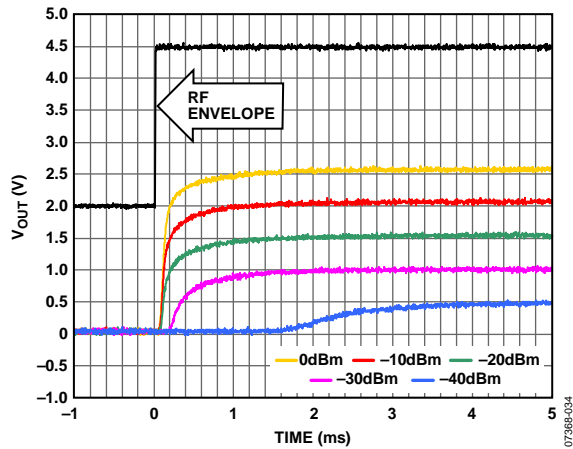


Figure 22. Output Response to RF Burst Input, Carrier Frequency at 2.14 GHz,  $C_{LPF} = 0.1\text{ }\mu\text{F}$ ,  $C_{HPF} = \text{Open}$ , Rising Edge

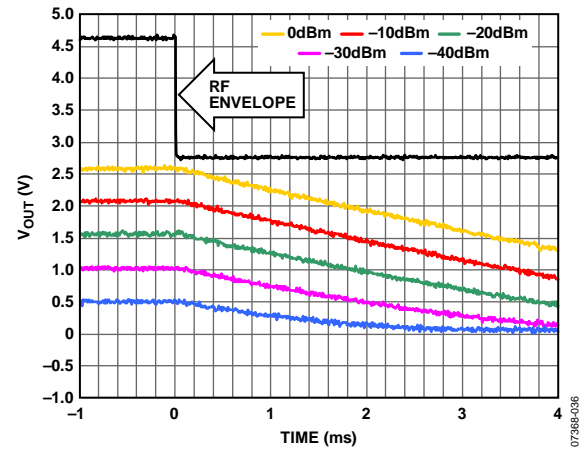


Figure 25. Output Response to RF Burst Input, Carrier Frequency at 2.14 GHz,  $C_{LPF} = 0.1\text{ }\mu\text{F}$ ,  $C_{HPF} = \text{Open}$ , Falling Edge

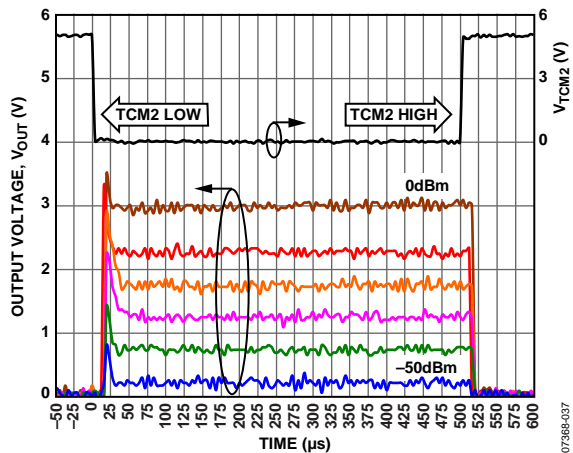


Figure 23. Output Response Using Power-Down Mode for Various RF Input Levels Carrier Frequency at 2.14 GHz,  $C_{LPF} = 470\text{ pF}$ ,  $C_{HPF} = 220\text{ pF}$

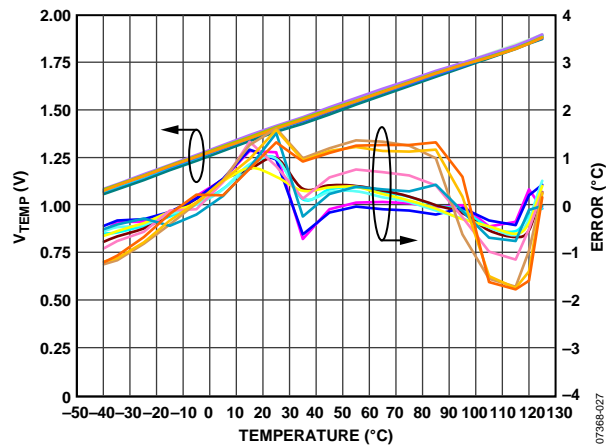


Figure 26.  $V_{TEMP}$  and Error with Respect to Straight Line vs. Temperature for Eleven Devices

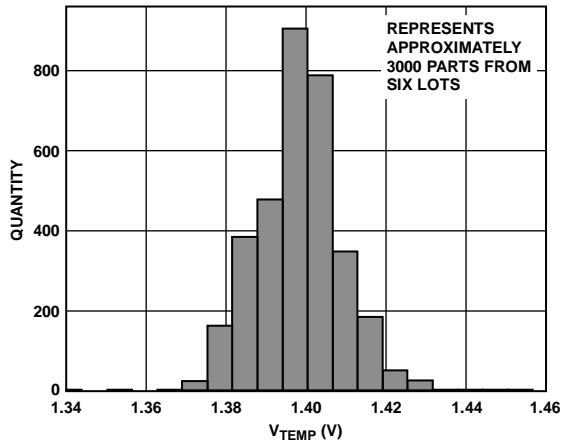


Figure 27. Distribution of  $V_{TEMP}$  Voltage at 25°C, No RF Input

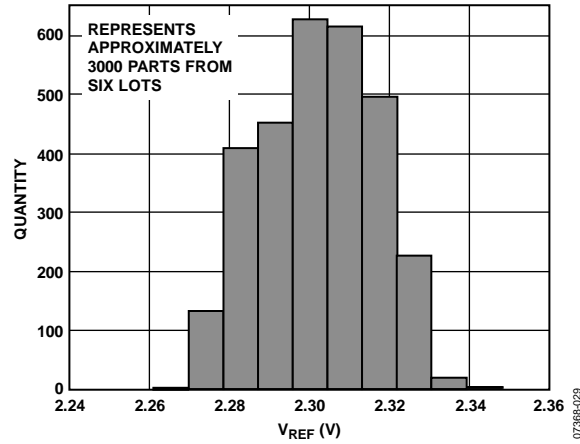


Figure 30. Distribution of  $V_{REF}$ , 25°C, No RF Input

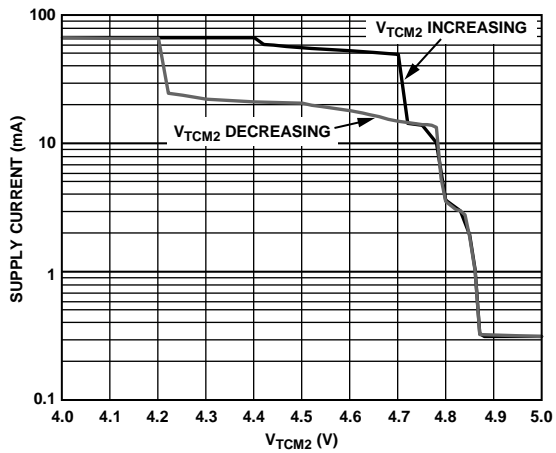


Figure 28. Supply Current vs.  $V_{TCM2}$

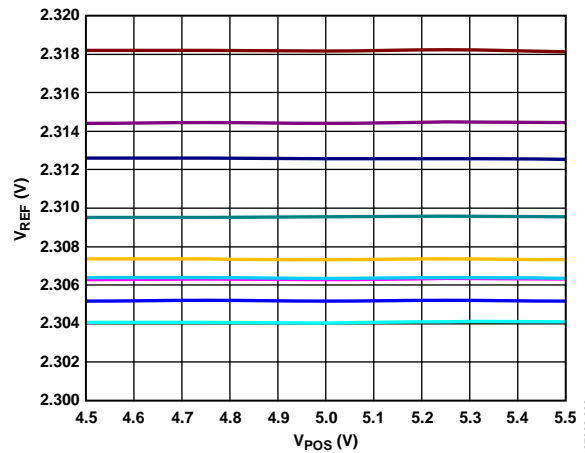


Figure 31. Change in  $V_{REF}$  with  $V_{POS}$  for Nine Devices

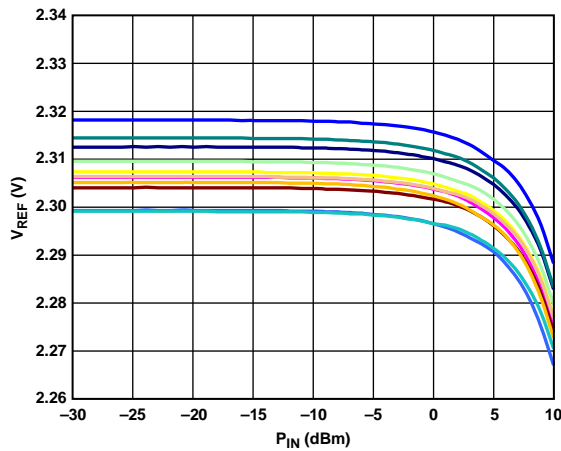


Figure 29. Change in  $V_{REF}$  with Input Amplitude for Eleven Devices

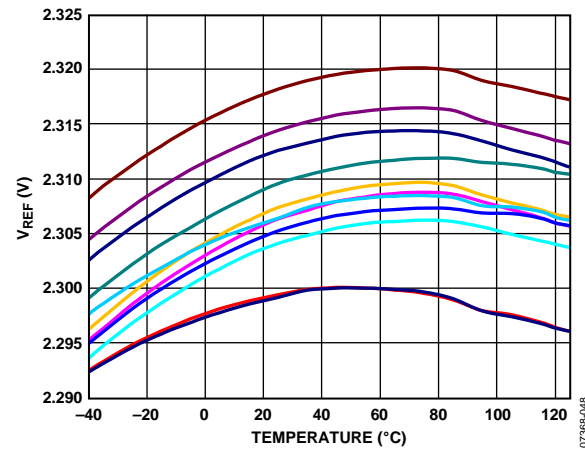


Figure 32. Change in  $V_{REF}$  with Temperature for Eleven Devices

## THEORY OF OPERATION

The computational core of the AD8363 is a high performance AGC loop. As shown in Figure 33, the AGC loop comprises a wide bandwidth variable gain amplifier (VGA), square law detectors, an amplitude target circuit, and an output driver. For a more detailed description of the functional blocks, see the AD8362 data sheet.

The nomenclature used in this data sheet to distinguish between a pin name and the signal on that pin is as follows:

- The pin name is all uppercase (for example, VPOS, COMM, and VOUT).
- The signal name or a value associated with that pin is the pin mnemonic with a partial subscript (for example,  $C_{LPF}$ ,  $C_{HPF}$ , and  $V_{OUT}$ ).

### SQUARE LAW DETECTOR AND AMPLITUDE TARGET

The VGA gain has the form

$$G_{SET} = G_O \exp(-V_{SET}/V_{GNS}) \quad (1)$$

where:

$G_O$  is the basic fixed gain.

$V_{GNS}$  is a scaling voltage that defines the gain slope (the decibel change per voltage). The gain decreases with increasing  $V_{SET}$ .

The VGA output is

$$V_{SIG} = G_{SET} \times RF_{IN} = G_O \times RF_{IN} \exp(V_{SET}/V_{GNS}) \quad (2)$$

where  $RF_{IN}$  is the ac voltage applied to the input terminals of the AD8363.

The output of the VGA,  $V_{SIG}$ , is applied to a wideband square law detector. The detector provides the true rms response of the RF input signal, independent of waveform. The detector output,  $I_{SQR}$ , is a fluctuating current with positive mean value. The difference between  $I_{SQR}$  and an internally generated current,  $I_{TGT}$ , is integrated by  $C_F$  and the external capacitor attached to the CLPF pin at the summing node.  $C_F$  is an on-chip 25 pF filter capacitor, and  $C_{LPF}$ , the external capacitance connected to the CLPF pin, can be used to arbitrarily increase the averaging time while trading off with the response time. When the AGC loop is at equilibrium

$$\text{Mean}(I_{SQR}) = I_{TGT} \quad (3)$$

This equilibrium occurs only when

$$\text{Mean}(V_{SIG}^2) = V_{TGT}^2 \quad (4)$$

where  $V_{TGT}$  is the voltage presented at the VTGT pin. This pin can conveniently be connected to the VREF pin through a voltage divider to establish a target rms voltage  $V_{ATG}$  of ~70 mV rms, when  $V_{TGT} = 1.4$  V.

Because the square law detectors are electrically identical and well matched, process and temperature dependent variations are effectively cancelled.

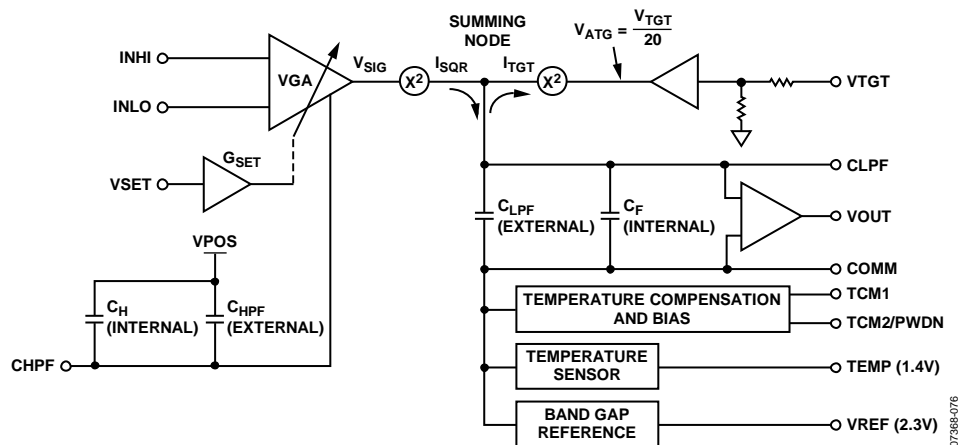


Figure 33. Simplified Architecture Details

By forcing the previous identity through varying the VGA setpoint, it is apparent that

$$\text{RMS}(V_{\text{SIG}}) = \sqrt{\text{Mean}(V_{\text{SIG}}^2)} = \sqrt{(V_{\text{ATG}})^2} = V_{\text{ATG}} \quad (5)$$

Substituting the value of  $V_{\text{SIG}}$  from Equation 2 results in

$$\text{RMS}(G_0 \times \text{RF}_{\text{IN}} \exp(-V_{\text{SET}}/V_{\text{GNS}})) = V_{\text{ATG}} \quad (6)$$

When connected as a measurement device,  $V_{\text{SET}} = V_{\text{OUT}}$ . Solving for  $V_{\text{OUT}}$  as a function of  $\text{RF}_{\text{IN}}$

$$V_{\text{OUT}} = V_{\text{SLOPE}} \times \log_{10}(\text{RMS}(\text{RF}_{\text{IN}})/V_Z) \quad (7)$$

where:

$V_{\text{SLOPE}}$  is 1 V/decade (or 50 mV/dB).

$V_Z$  is the intercept voltage.

When  $\text{RMS}(\text{RF}_{\text{IN}}) = V_Z$ , because  $\log_{10}(1) = 0$ , this implies that  $V_{\text{OUT}} = 0$  V, making the intercept the input that forces  $V_{\text{OUT}} = 0$  V.  $V_Z$  has been fixed to approximately 280  $\mu\text{V}$  (approximately -58 dBm, referred to 50  $\Omega$ ) with a CW signal at 100 MHz. In reality, the AD8363 does not respond to signals less than  $\sim -56$  dBm. This means that the intercept is an extrapolated value outside the operating range of the device.

If desired, the effective value of  $V_{\text{SLOPE}}$  can be altered by using a resistor divider between  $V_{\text{OUT}}$  and  $V_{\text{SET}}$ . (Refer to the Output Voltage Scaling section for more information.)

In most applications, the AGC loop is closed through the setpoint interface and the  $V_{\text{SET}}$  pin. In measurement mode,  $V_{\text{OUT}}$  is directly connected to  $V_{\text{SET}}$ . (See the Measurement Mode Basic Connections section for more information.) In controller mode, a control voltage is applied to  $V_{\text{SET}}$  and the  $V_{\text{OUT}}$  pin typically drives the control input of an amplification or attenuation system. In this case, the voltage at the  $V_{\text{SET}}$  pin forces a signal amplitude at the RF inputs of the AD8363 that balances the system through feedback. (See the Controller Mode Basic Connections section for more information.)

## RF INPUT INTERFACE

Figure 34 shows the connections of the RF inputs within the AD8363. The input impedance is set primarily by an internal 50  $\Omega$  resistor connected between INHI and INLO. A dc level of approximately half the supply voltage on each pin is established internally. Either the INHI pin or the INLO pin can be used as the single-ended RF input pin. (See the Choice of RF Input Pin section.) If the dc levels at these pins are disturbed, performance is compromised; therefore, signal coupling capacitors must be connected from the input signal to INHI and INLO. The input signal high-pass corner formed by the coupling capacitors and the internal resistances is

$$f_{\text{HIGH-PASS}} = 1/(2 \times \pi \times 50 \times C) \quad (8)$$

where  $C$  is in farads and  $f_{\text{HIGH-PASS}}$  is in hertz. The input coupling capacitors must be large enough in value to pass the input signal frequency of interest. The other input pin should be RF ac-coupled to common (ground).

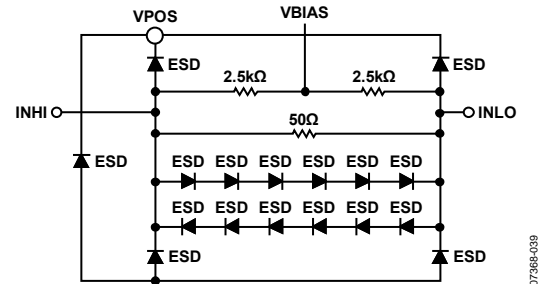


Figure 34. RF Inputs Simplified Schematic

Extensive ESD protection is employed on the RF inputs, which limits the maximum possible input amplitude to the AD8363.

## CHOICE OF RF INPUT PIN

The dynamic range of the AD8363 can be optimized by choosing the correct RF input pin for the intended frequency of operation. Using INHI (Pin 14), users can obtain the best dynamic range at frequencies up to 2.6 GHz. Above 2.6 GHz, it is recommended that INLO (Pin 15) be used. At 2.6 GHz, the performance obtained at the two inputs is approximately equal.

The AD8363 was designed with a single-ended RF drive in mind. A balun can be used to drive INHI and INLO differentially, but it is not necessary, and it does not result in improved dynamic range.

## SMALL SIGNAL LOOP RESPONSE

The AD8363 uses a VGA in a loop to force a squared RF signal to be equal to a squared dc voltage. This nonlinear loop can be simplified and solved for a small signal loop response. The low-pass corner pole is given by

$$\text{Freq}_{\text{LP}} \approx 1.83 \times I_{\text{TGT}}/(C_{\text{LPF}}) \quad (9)$$

where:

$I_{\text{TGT}}$  is in amperes.

$C_{\text{LPF}}$  is in farads.

$\text{Freq}_{\text{LP}}$  is in hertz.

$I_{\text{TGT}}$  is derived from  $V_{\text{TGT}}$ ; however,  $I_{\text{TGT}}$  is a squared value of  $V_{\text{TGT}}$  multiplied by a transresistance, namely

$$I_{\text{TGT}} = g_m \times V_{\text{TGT}}^2 \quad (10)$$

$g_m$  is approximately 18.9  $\mu\text{S}$ , so with  $V_{\text{TGT}}$  equal to the typically recommended 1.4 V,  $I_{\text{TGT}}$  is approximately 37  $\mu\text{A}$ . The value of this current varies with temperature; therefore, the small signal pole varies with temperature. However, because the RF squaring circuit and dc squaring circuit track with temperature, there is no temperature variation contribution to the absolute value of  $V_{\text{OUT}}$ .

For CW signals,

$$\text{Freq}_{\text{LP}} \approx 67.7 \times 10^{-6}/(C_{\text{LPF}}) \quad (11)$$

However, signals with large crest factors include low pseudorandom frequency content that either needs to be filtered out or sampled and averaged out. See the Choosing a Value for CLPF section for more information.

## TEMPERATURE SENSOR INTERFACE

The AD8363 provides a temperature sensor output with an output voltage scaling factor of approximately 5 mV/°C. The output is capable of sourcing 4 mA and sinking 50  $\mu$ A maximum at temperatures at or above 25°C. If additional current sink capability is desired, an external resistor can be connected between the TEMP and COMM pins. The typical output voltage at 25°C is approximately 1.4 V.

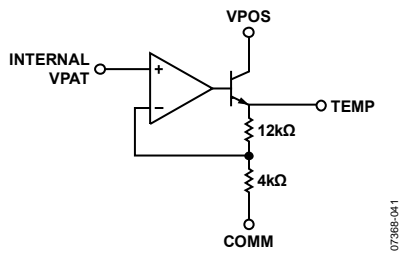


Figure 35. TEMP Interface Simplified Schematic

## VREF INTERFACE

The VREF pin provides an internally generated voltage reference. The  $V_{REF}$  voltage is a temperature stable 2.3 V reference that is capable of sourcing 4 mA and sinking 50  $\mu$ A maximum at temperatures at or above 25°C. An external resistor can be connected between the VREF and COMM pins to provide additional current sink capability. The voltage on this pin can be used to drive the TCM1, TCM2/PWDN, and VTGT pins, if desired.

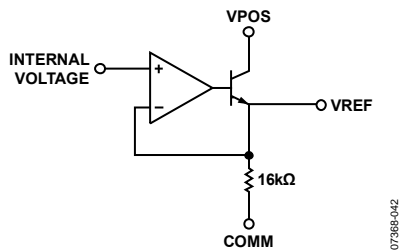


Figure 36. VREF Interface Simplified Schematic

## TEMPERATURE COMPENSATION INTERFACE

Proprietary techniques are used to maximize the temperature stability of the AD8363. For optimal performance, the output temperature drift must be compensated for using the TCM1 and TCM2/PWDN pins. The absolute value of compensation varies with frequency and  $V_{TGT}$ . Table 4 shows the recommended voltages for the TCM1 and TCM2/PWDN pins to maintain the best temperature drift error over the rated temperature range ( $-40^{\circ}\text{C} < T_A < 85^{\circ}\text{C}$ ) when driven single-ended and using a  $V_{TGT} = 1.4$  V.

Table 4. Recommended Voltages for TCM1 and TCM2/PWDN

Frequency	TCM1 (V)	TCM2/PWDN (V)
100 MHz	0.47	1.0
900 MHz	0.5	1.2
1.9 GHz	0.52	0.51
2.14 GHz	0.52	0.6
2.6 GHz	0.54	1.1
3.8 GHz	0.56	1.0
5.8 GHz	0.88	1.0

The values in Table 4 were chosen to give the best drift performance at the high end of the usable dynamic range over the  $-40^{\circ}\text{C}$  to  $+85^{\circ}\text{C}$  temperature range.

Compensating the device for the temperature drift using TCM1 and TCM2/PWDN allows for great flexibility and the user may wish to modify these values to optimize for another amplitude point in the dynamic range, for a different temperature range, or for an operating frequency other than those shown in Table 4.

To find a new compensation point,  $V_{TCM1}$  and  $V_{TCM2}$  can be swept while monitoring  $V_{OUT}$  over the temperature at the frequency and amplitude of interest. The optimal voltages for  $V_{TCM1}$  and  $V_{TCM2}$  to achieve minimum temperature drift at a given power and frequency are the values of  $V_{TCM1}$  and  $V_{TCM2}$  where  $V_{OUT}$  has minimum movement. See the AD8364 and ADL5513 data sheets for more information.

Varying  $V_{TCM1}$  and  $V_{TCM2}$  has only a very slight effect on  $V_{OUT}$  at device temperatures near 25°C; however, the compensation circuit has more and more effect, and is more and more necessary for best temperature drift performance, as the temperature departs farther from 25°C.

Figure 37 shows the effect on temperature drift performance at 25°C and 85°C as  $V_{TCM1}$  is varied but  $V_{TCM2}$  is held constant at 0.6 V.

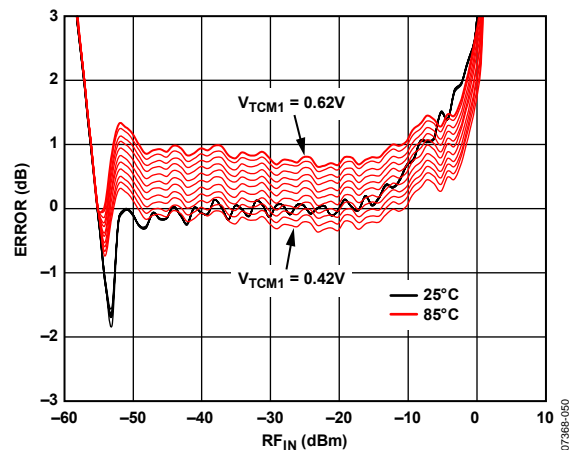


Figure 37. Error vs. Input Amplitude over Stepped  $V_{TCM1}$  Values, 25°C and 85°C, 2.14 GHz,  $V_{TCM2} = 0.6$  V

TCM1 primarily adjusts the intercept of the AD8363 at temperature. In this way, TCM1 can be thought of as a coarse adjustment to the compensation. Conversely, TCM2 performs a fine adjustment. For this reason, it is advised that when searching for compensation with  $V_{TCM1}$  and  $V_{TCM2}$ , that  $V_{TCM1}$  be adjusted first, and when best performance is found,  $V_{TCM2}$  can then be adjusted for optimization.

It is evident from Figure 37 that the temperature compensation circuit can be used to adjust for the lowest drift at any input amplitude of choice. Though not shown in Figure 37, a similar analysis can simultaneously be performed at  $-40^{\circ}\text{C}$ , or any other temperature within the operating range of the AD8363.

Performance varies slightly from device to device; therefore, optimal  $V_{TCM1}$  and  $V_{TCM2}$  values must be arrived at statistically



over a population of devices to be useful in mass production applications.

The TCM1 and TCM2 pins have high input impedances, approximately 5 kΩ and 500 kΩ, respectively, and can be conveniently driven from an external source or from a fraction of VREF by using a resistor divider. VREF does change slightly with temperature and RF input amplitude (see Figure 32 and Figure 29); however, the amount of change is unlikely to result in a significant effect on the final temperature stability of the RF measurement system.

Figure 38 shows a simplified schematic representation of TCM1. See the Power-Down Interface section for the TCM2 interface.

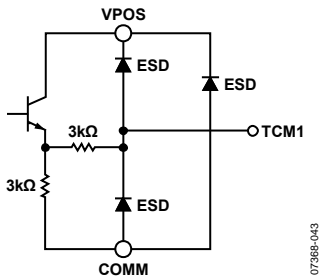


Figure 38. TCM1 Interface Simplified Schematic

**POWER-DOWN INTERFACE**

The quiescent and disabled currents for the AD8363 at 25°C are approximately 60 mA and 300 μA, respectively. The dual function pin, TCM2/PWDN, is connected to a temperature compensation circuit as well as a power-down circuit. Typically, when PWDN is greater than  $V_{POS} - 0.1$  V, the device is fully powered down. Figure 28 shows this characteristic as a function of  $V_{PWDN}$ . Note that because of the design of this section of the AD8363, as  $V_{TCM2}$  passes through a narrow range at ~4.5 V (or  $\sim V_{POS} - 0.5$  V), the TCM2/PWDN pin sinks approximately 750 μA. The source used to disable the AD8363 must have a sufficiently high current capability for this reason. Figure 23 shows the typical response times for various RF input levels. The output reaches within 0.1 dB of its steady-state value in approximately 35 μs; however, the reference voltage is available to full accuracy in a much shorter time. This wake-up response varies depending on the input coupling and the capacitances,  $C_{HPF}$  and  $C_{LPF}$ .

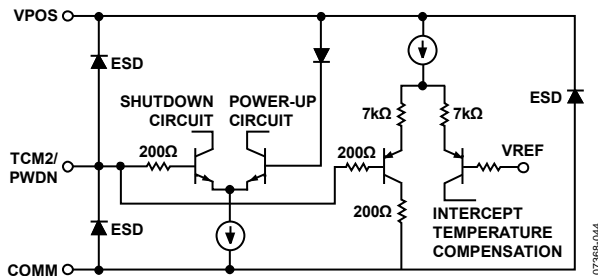


Figure 39. PWDN Interface Simplified Schematic

**VSET INTERFACE**

The VSET interface has a high input impedance of 72 kΩ. The voltage at VSET is converted to an internal current used to set the internal VGA gain. The VGA attenuation control is approximately 19 dB/V.

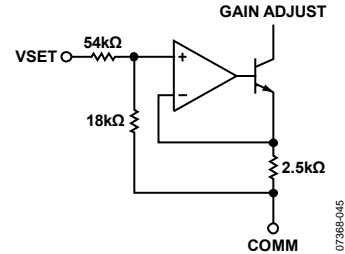


Figure 40. VSET Interface Simplified Schematic

**OUTPUT INTERFACE**

The output driver used in the AD8363 is different from the output stage on the AD8362. The AD8363 incorporates rail-to-rail output drivers with pull-up and pull-down capabilities. The closed-loop -3 dB bandwidth of the VOUT buffer with no load is approximately 58 MHz with a single-pole roll-off of -20 dB/dec. The output noise is approximately 45 nV/√Hz at 100 kHz, which is independent of  $C_{LPF}$  due to the architecture of the AD8363. VOUT can source and sink up to 10 mA. There is an internal load between VOUT and COMM of 2.5 kΩ.

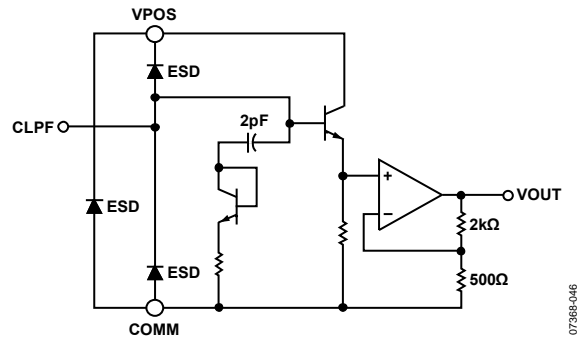


Figure 41. VOUT Interface Simplified Schematic

**VTGT INTERFACE**

The target voltage can be set with an external source or by connecting the VREF pin (nominally 2.3 V) to the VTGT pin through a resistive voltage divider. With 1.4 V on the VTGT pin, the rms voltage that must be provided by the VGA to balance the AGC feedback loop is  $1.4 \text{ V} \times 0.05 = 70 \text{ mV rms}$ . Most of the characterization information in this data sheet was collected at  $V_{TGT} = 1.4 \text{ V}$ . Voltages higher and lower than this can be used; however, doing so increases or decreases the gain at the internal squaring cell, which results in a corresponding increase or decrease in intercept. This in turn affects the sensitivity and the usable measurement range. Because the gain of the squaring cell varies with temperature, oscillations or a loss in measurement range can result. For these reasons, do not reduce  $V_{TGT}$  below 1.3 V.

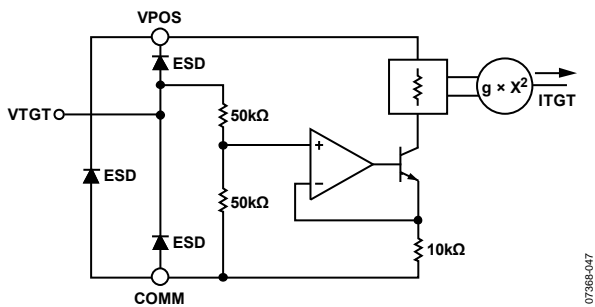


Figure 42. VTGT Interface Simplified Schematic

**MEASUREMENT MODE BASIC CONNECTIONS**

The AD8363 requires a single supply of nominally 5 V. The supply is connected to the two supply pins, VPOS. Decouple the pins using two capacitors with values equal or similar to those shown in Figure 43. These capacitors must provide a low impedance over the full frequency range of the input, and they should be placed as close as possible to the VPOS pins. Use two different capacitor values in parallel to provide a broadband ac short to ground.

Input signals can be applied differentially or single-ended; however, in both cases, the input impedance is 50 Ω. Most performance information in this data sheet was derived with a single-ended drive. The optimal measurement range is achieved using a single-ended drive on the INHI pin at frequencies below 2.6 GHz (as shown in Figure 43), and likewise, optimal performance is achieved using the INLO pin above 2.6 GHz (similar to Figure 43; except INLO is ac-coupled to the input and INHI is ac-coupled to ground).

The AD8363 is placed in measurement mode by connecting VOUT to VSET. This closes the AGC loop within the device with  $V_{OUT}$  representing the VGA control voltage, which is required to present the correct rms voltage at the input of the internal square law detector.

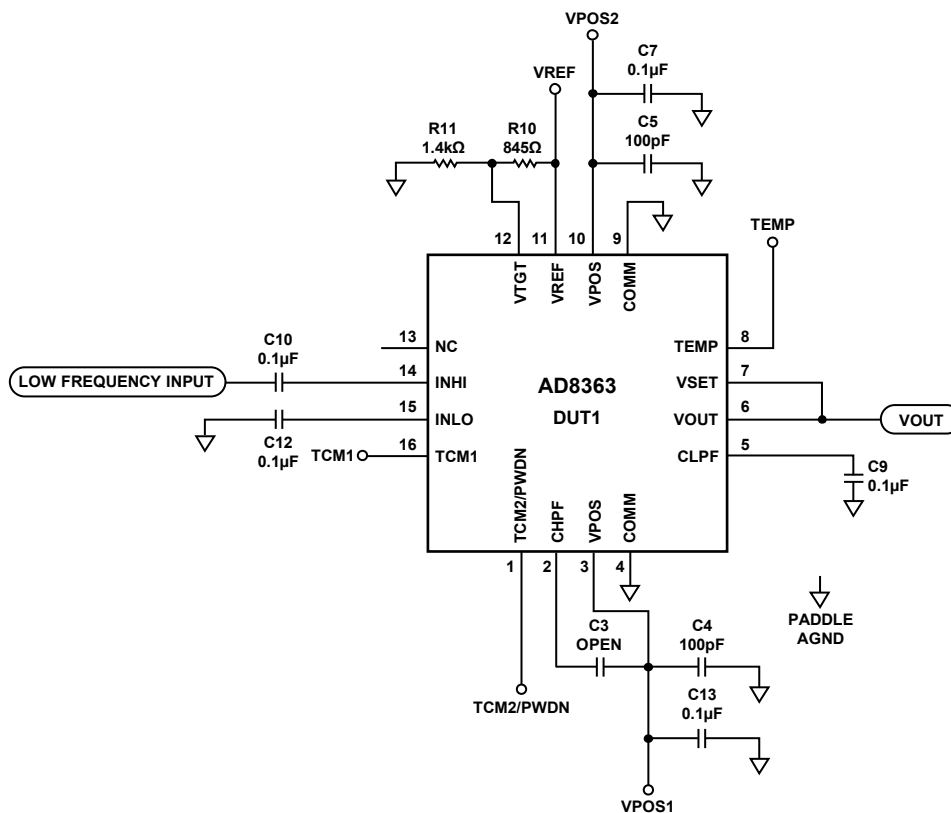


Figure 43. Measurement Mode Basic Connections

## SYSTEM CALIBRATION AND ERROR CALCULATION

The measured transfer function of the AD8363 at 1.9 GHz is shown in Figure 44, which contains plots of both output voltage vs. input amplitude (power) and calculated error vs. input level. As the input level varies from  $-55$  dBm to  $+0$  dBm, the output voltage varies from  $\sim 0$  V to  $\sim 3.1$  V.

Because slope and intercept vary from device to device, board-level calibration must be performed to achieve high accuracy. The equation for the idealized output voltage can be written as

$$V_{OUT(IDEAL)} = Slope \times (P_{IN} - Intercept) \quad (12)$$

where:

*Slope* is the change in output voltage divided by the change in input power (dB).

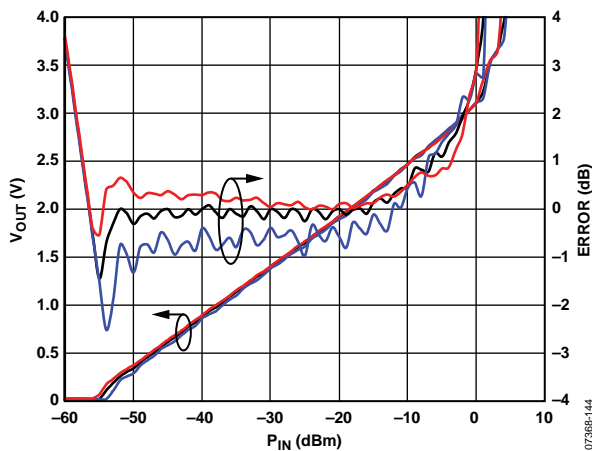


Figure 44. 1.9 GHz Transfer Function and Linearity Error using a Two-Point Calibration (Calibration Points  $-20$  dBm and  $-40$  dBm)

*Intercept* is the calculated input power level at which the output voltage would equal  $0$  V (note that *Intercept* is an extrapolated theoretical value not a measured value).

In general, calibration, which establishes the *Slope* and *Intercept*, is performed during equipment manufacture by applying two or more known signal levels to the input of the AD8363 and measuring the corresponding output voltages. The calibration points are generally chosen within the linear-in-dB operating range of the device.

With a two-point calibration, the slope and intercept are calculated as follows:

$$Slope = (V_{OUT1} - V_{OUT2}) / (P_{IN1} - P_{IN2}) \quad (13)$$

$$Intercept = P_{IN1} - (V_{OUT1} / Slope) \quad (14)$$

After the slope and intercept are calculated and stored in non-volatile memory during equipment calibration, an equation can be used to calculate an unknown input power based on the output voltage of the detector.

$$P_{IN} (Unknown) = (V_{OUT(MEASURED)} / Slope) + Intercept \quad (15)$$

The log conformance error is the difference between this straight line and the actual performance of the detector.

$$Error (dB) = (V_{OUT(MEASURED)} - V_{OUT(IDEAL)}) / Slope \quad (16)$$

Figure 44 includes a plot of this error when using a two-point calibration (calibration points are  $-20$  dBm and  $-40$  dBm). The error at the calibration points is equal to  $0$  by definition.

The residual nonlinearity of the transfer function that is apparent in the two-point calibration error plot can be reduced by increasing the number of calibration points. Figure 45 shows the post-calibration error plots for three-point calibration. With a multipoint calibration, the transfer function is segmented, with each segment having its own slope and intercept. During calibration, multiple known power levels are applied, and multiple voltages are measured. When the equipment is in operation, the measured voltage from the detector is first used to determine which of the stored slope and intercept calibration coefficients are to be used. Then the unknown power level is calculated by inserting the appropriate slope and intercept into Equation 15.

Figure 45 shows the output voltage and error at  $25^{\circ}\text{C}$  and over temperature when a three-point calibration is used (calibration points are  $0$  dBm,  $-10$  dBm and  $-40$  dBm). When choosing calibration points, there is no requirement for, or value in equal spacing between the points. There is also no limit to the number of calibration points used.

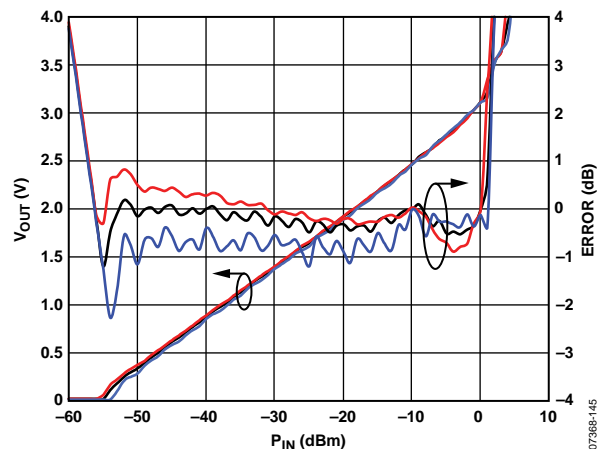


Figure 45. 1.9 GHz Transfer Function and Error at  $+25^{\circ}\text{C}$ ,  $-40^{\circ}\text{C}$ , and  $+85^{\circ}\text{C}$  Using a Three-Point Calibration ( $0$  dBm,  $-10$  dBm and  $-40$  dBm)

The  $-40^{\circ}\text{C}$  and  $+85^{\circ}\text{C}$  error plots in Figure 44 and Figure 45 are generated using the  $25^{\circ}\text{C}$  calibration coefficients. This is consistent with equipment calibration in a mass production environment where calibration at just a single temperature is practical.

## OPERATION TO $125^{\circ}\text{C}$

The AD8363 operates up to  $125^{\circ}\text{C}$  with slightly degraded performance. Figure 46 shows the typical operation (Errors are plotted using two-point calibration) at  $125^{\circ}\text{C}$  as compared to other temperatures using the TCM1 and TCM2 values in Table 4. Temperature compensation can be optimized for operation above  $85^{\circ}\text{C}$  by modifying the voltages on the TCM1 and TCM2 pins from those shown in Table 4.

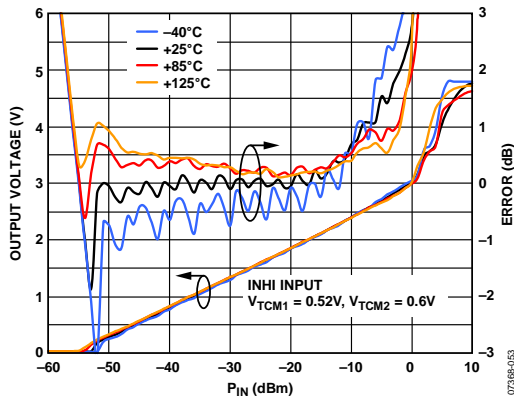


Figure 46.  $V_{OUT}$  and Log Conformance Error vs. Input Amplitude at 2.14 GHz,  $-40^{\circ}\text{C}$  to  $+125^{\circ}\text{C}$

## OUTPUT VOLTAGE SCALING

The output voltage range of the AD8363 (nominally 0 V to 3.5 V) can be easily increased or decreased. There are a number of situations where adjustment of the output scaling makes sense. For example, if the AD8363 is driving an analog-to-digital converter (ADC) with a 0 V to 5 V input range, it makes sense to increase the detector's nominal maximum output voltage of 3.5 V so that it is closer to 5 V. This makes better use of the input range of the ADC and maximizes the resolution of the system in terms of bits/dB.

If only a part of the RF input power range of the AD8363 is being used (for example,  $-10$  dBm to  $-40$  dBm), it may make sense to increase the scaling so that this reduced input range fits into the available output swing of the AD8363 (0 V to 4.8 V).

The output swing can be reduced by adding a voltage divider on the output pin, as shown in Figure 47 (with VOUT connected directly to VSET and a resistor divider on VOUT). Figure 47 also shows how the output voltage swing can be increased using a technique that is analogous to setting the gain of an op amp in noninverting mode. With the VSET pin being the equivalent of the inverting input of the op amp, a resistor divider is connected between VOUT and VSET.

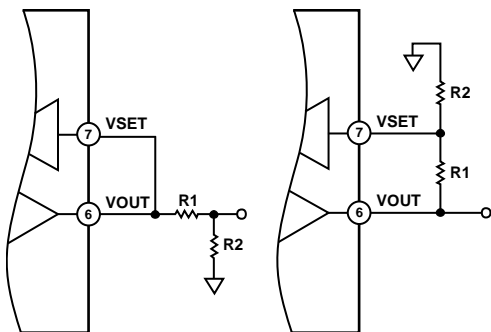


Figure 47. Decreasing and Increasing Slope

Equation 17 is the general function that governs this.

$$RI = (R2 \parallel R_{IN}) \left( \frac{V'_O}{V_O} - 1 \right) \quad (17)$$

where:

$V_O$  is the nominal maximum output voltage (see Figure 4 through Figure 18).

$V'_O$  is the new maximum output voltage (for example, up to 4.8 V).

$R_{IN}$  is the VSET input resistance (72 k $\Omega$ ).

When choosing R1 and R2, attention must be paid to the current drive capability of the VOUT pin and the input resistance of the VSET pin. The choice of resistors should not result in excessive current draw out of VOUT. However, making R1 and R2 too large is also problematic. If the value of R2 is compatible with the 72 k $\Omega$  input resistance of the VSET input, this input resistance, which varies slightly from device to device, contributes to the resulting slope and output voltage. In general, the value of R2 should be at least ten times smaller than the input resistance of VSET. Values for R1 and R2 should, therefore, be in the 1 k $\Omega$  to 5 k $\Omega$  range.

It is also important to take into account device-to-device and frequency variation in output swing along with the AD8363 output stage's maximum output voltage of 4.8 V. The  $V_{OUT}$  distribution is well characterized at the bands of major frequencies in the Typical Performance Characteristics section (Figure 3 to Figure 18).

## OFFSET COMPENSATION, MINIMUM $C_{LPF}$ , AND MAXIMUM $C_{HPF}$ CAPACITANCE VALUES

An offset-compensation loop is used to eliminate small dc offsets within the internal VGA as shown in Figure 48. The high-pass corner frequency of this loop is set to about 1 MHz using an on-chip 25 pF capacitor. Because input signals that are below 1 MHz are interpreted as unwanted offset voltages, this restricts the operating frequency range of the device. To operate the AD8363 at lower frequencies (than 1 MHz), the high-pass corner frequency must be reduced by connecting a capacitor between CHPF and VPOS.

Internal offset voltages vary depending on the gain at which the VGA is operating and, therefore, on the input signal amplitude. When a large  $C_{HPF}$  value is used, the offset correction process can lag the more rapid changes in the gain of the VGA, which can increase the time required for the loop to fully settle for a given steady input amplitude. This can manifest itself in a jumpy, seemingly oscillatory response of the AD8363.

Care should therefore be taken in choosing  $C_{HPF}$  and  $C_{LPF}$  because there is a potential to create oscillations. In general, make the capacitance on the CLPF pin as large as possible; there is no maximum on the amount of capacitance that can be added to this pin. At high frequencies, there is no need for an external capacitor on the CHPF pin; therefore, the pin can be left open. However, when trying to get a fast response time and/or when working at low frequencies, extra care in choosing the proper capacitance values for  $C_{HPF}$  and  $C_{LPF}$  is prudent. With the gain control pin (VSET) connected to VOUT,  $V_{SET}$  can slew at a rate determined by the on-chip squaring cell and  $C_{LPF}$ . When  $V_{SET}$  is changing with time, the dc offsets in the VGA also vary with

time. The speed at which  $V_{SET}$  slews can create a time varying offset that falls within the high-pass corner set by  $C_{HPF}$ . Therefore, in measurement mode, take care to set  $C_{LPF}$  appropriately to reduce the slew. It is also worth noting that most of the typical performance data was derived with  $C_{LPF} = 3.9$  nF and  $C_{HPF} = 2.7$  nF and with a CW waveform.

The minimum appropriate  $C_{LPF}$  based on slew rate limitations is as follows

$$C_{LPF} > 20 \times 10^{-3} / FREQ_{RFIN} \quad (18)$$

where:

$C_{LPF}$  is in farads.

$FREQ_{RFIN}$  is in hertz.

This takes into account the on-chip 25 pF capacitor,  $C_F$ , in parallel with  $C_{LPF}$ . However, because there are other internal device time delays that affect loop stability, use a minimum  $C_{LPF}$  of 390 pF.

The minimum appropriate  $C_{HPF}$  for a given high-pass pole frequency is

$$C_{HPF} = 29.2 \times 10^{-6} / FHP_{POLE} - 25 \text{ pF} \quad (19)$$

where  $FHP_{POLE}$  is in hertz.

The subtraction of 25 pF is a result of the on-chip 25 pF capacitor in parallel with the external  $C_{HPF}$ . Typically, choose  $C_{HPF}$  to give a pole (3 dB corner) at least 1 decade below the desired signal frequency. Note that the high pass corner of the offset compensation system is approximately 1 MHz without an external  $C_{HPF}$ ; therefore, adding an external capacitor lowers the corner frequency.

The following example illustrates the proper selection of the input coupling capacitors, minimum  $C_{LPF}$ , and maximum  $C_{HPF}$  when using the AD8363 in measurement mode for a 1 GHz input signal.

1. Choose the input coupling capacitors that have a 3 dB corner at least one decade below the input signal frequency. From Equation 8,  $C > 10 / (2 \times \pi \times RF_{IN} \times 50) = 32$  pF minimum. According to this calculation, 32 pF is sufficient; however, the input coupling capacitors should be a much larger value, typically 0.1  $\mu$ F. The offset compensation circuit, which is connected to  $CHPF$ , should be the true determinant of the system high-pass corner frequency and not the input coupling capacitors. With 0.1  $\mu$ F coupling capacitors, signals as low as 32 kHz can couple to the input, which is well below the system high-pass frequency.
2. Choose  $C_{LPF}$  to reduce instabilities due to  $VSET$  slew rate. See Equation 18, where  $FREQ_{RFIN} = 1$  GHz, and this results in  $C_{LPF} > 20$  pF. However, as previously mentioned, values below 390 pF are not recommended. For this reason, a 470 pF capacitor was chosen. In addition, if fast response times are not required, an even larger  $C_{LPF}$  value than given here should be chosen.

3. Choose  $C_{HPF}$  to set a 3 dB corner to the offset compensation system. See Equation 19, where  $FHP_{POLE}$  is in this case 100 MHz, one decade below the desired signal. This results in a negative number and, obviously, a negative value is not practical. Because the high-pass corner frequency is already 1 MHz, this result simply illustrates that the appropriate solution is to use no external  $C_{HPF}$  capacitor.

Note that per Equation 9

$$Freq_{LP} \approx 1.83 \times I_{TGT} / (C_{LPF})$$

A  $C_{LPF}$  of 470 pF results in a small signal low-pass corner frequency of approximately 144 kHz. This reflects the bandwidth of the measurement system, and how fast the user can expect changes on the output. It does not imply any limitations on the input RF carrier frequency.

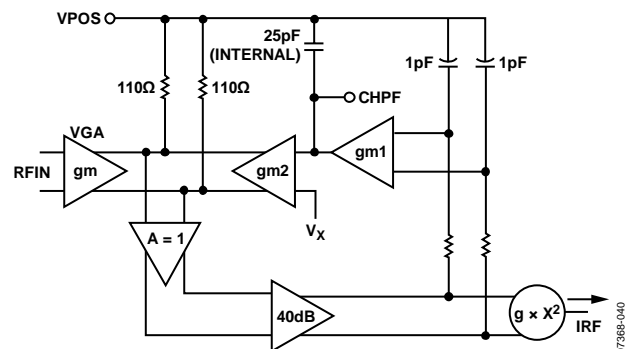


Figure 48. Offset Compensation Circuit

## CHOOSING A VALUE FOR $C_{LPF}$

The Small Signal Loop Response section and the Offset Compensation, Minimum  $C_{LPF}$ , and Maximum  $C_{HPF}$  Capacitance Values section discussed how to choose the minimum value capacitance for  $C_{LPF}$  based on a minimum capacitance of 390 pF, slew rate limitation, and frequency of operation. Using the minimum value for  $C_{LPF}$  allows the quickest response time for pulsed type waveforms (such as WiMAX) but also allows the most residual ripple on the output caused by the pseudorandom modulation waveform. There is not a maximum for the capacitance that can be applied to the  $C_{LPF}$  pin, and in most situations, a large enough capacitor can be added to remove the residual ripple caused by the modulation and yet allow a fast enough response to changes in input power.

Figure 49 shows how residual ripple, rise time, and fall time vary with filter capacitance when the AD8363 is driven by a single carrier CDMA2000 9CH SR1 signal at 2.14 GHz. The rise time and fall time is based on a signal that is pulsed between no signal and 10 dBm but is faster if the input power change is less.

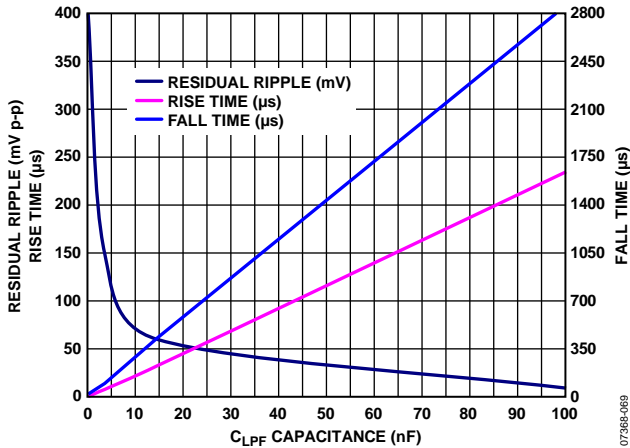


Figure 49. Residual Ripple, Rise Time, and Fall Time vs.  $C_{LPF}$  Capacitance, Single Carrier CDMA2000 9CH SR1 Signal at 2.14 GHz with 10 dBm Pulse

Table 5 shows the recommended values of  $C_{LPF}$  for popular modulation schemes. For nonpulsed waveforms, increase  $C_{LPF}$  until the residual output noise falls below 50 mV ( $\pm 0.5$  dB). In each case, the capacitor can be increased to further reduce the noise. A 10% to 90% step response to an input step is also listed. Where the increased response time is unacceptably high, reduce  $C_{LPF}$ , which increases the noise on the output. Due to the random nature of the output ripple, if it is sampled by an ADC, averaging in the digital domain further reduces the residual noise.

Table 5 gives  $C_{LPF}$  values to minimize noise while trying to keep a reasonable response time. For non-pulsed type waveforms, averaging is not required on the output. For pulsed waveforms, the smaller the noise, the less averaging is needed on the output.

System specifications determine the necessary rise time and fall time. For example, the suggested  $C_{LPF}$  value for WiMAX assumes that it is not necessary to measure the power in the preamble.

Figure 50 shows how the rise time cuts off the preamble. Note that the power in the preamble can be easily measured; however, the  $C_{LPF}$  value would have to be reduced slightly, and the noise in the main signal would increase.

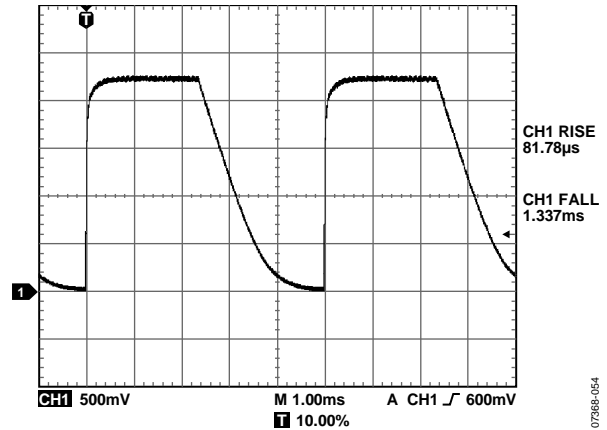


Figure 50. AD8363 Output Response to a WiMAX 802.16, 64 QAM, 256 Subcarriers, 10 MHz Bandwidth Signal with  $C_{LPF} = 0.027 \mu F$

As shown in Figure 49, the fall time for the AD8363 increases faster than the rise time with an increase in  $C_{LPF}$  capacitance. Some pulse-type modulation standards require a fast fall time as well as a fast rise time, and in all cases, less output ripple is desired. Placing an RC filter on the output reduces the ripple, according to the frequency content of the ripple and the poles and zeros of the filter. Using an RC output filter also changes the rise and fall time vs. the output ripple response as compared to increasing the  $C_{LPF}$  capacitance.

Table 5. Recommended  $C_{LPF}$  Values for Various Modulation Schemes

Modulation/Standard	Crest Factor (dB)	$C_{LPF}$	Residual Ripple (mV p-p)	Response Time (Rise/Fall) 10% to 90%
W-CDMA, 1Carrier, TM1-64	12	0.1 $\mu$ F	15	236 $\mu$ s/2.9 ms
W-CDMA, 1Carrier, TM1-64 (EVDO)	12	3900 pF	150	8.5 $\mu$ s/100 $\mu$ s
W-CDMA 4Carrier, TM1-64	11	0.1 $\mu$ F	8	240 $\mu$ s/2.99 ms
CDMA2000, 1Carrier, 9CH	9.1	0.1 $\mu$ F	10	210 $\mu$ s/3.1 ms
CDMA2000, 3Carrier, 9CH	11	0.1 $\mu$ F	13	215 $\mu$ s/3.14 ms
WiMAX 802.16, 64 QAM, 256 Subcarriers, 10 MHz Bandwidth	14	0.027 $\mu$ F	10	83 $\mu$ s/1.35 ms
6C TD-SCDMA	14	0.01 $\mu$ F	69	24 $\mu$ s/207 $\mu$ s
1C TD-SCDMA	11.4	0.01 $\mu$ F	75	24 $\mu$ s /198 $\mu$ s

Figure 51 shows the response for a 2.14 GHz pulsed signal, with  $C_{LPF} = 3900$  pF. The residual ripple from a single carrier CDMA2000 9CH SR1 signal is 150 mV p-p. (The ripple is not shown in Figure 51. The ripple was measured separately.) Figure 52 shows the response for a 2.14 GHz pulse signal with a  $C_{LPF}$  of 390 pF and an output filter that consists of a series 75  $\Omega$  resistor (closest to the output) followed by a 0.15  $\mu$ F capacitor to ground. The residual ripple for this configuration is also 150 mV p-p. Note that the rise time is faster and the fall time is slower when the larger  $C_{LPF}$  is used to obtain a 150 mV p-p ripple.

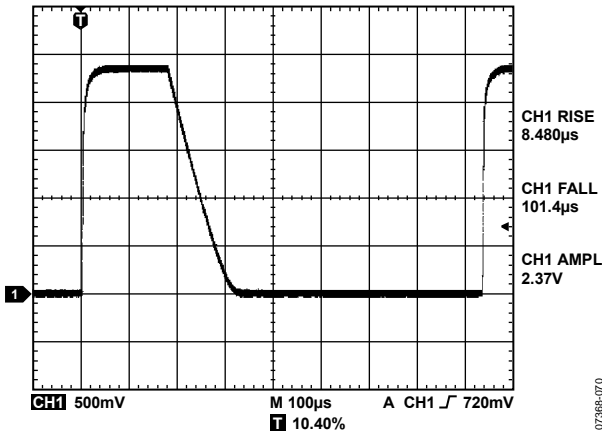


Figure 51. Pulse Response with  $C_{LPF} = 3900$  pF Resulting in a 150 mV p-p Ripple for a Single Carrier CDMA2000 9CH SR1 Signal at 2.14 GHz

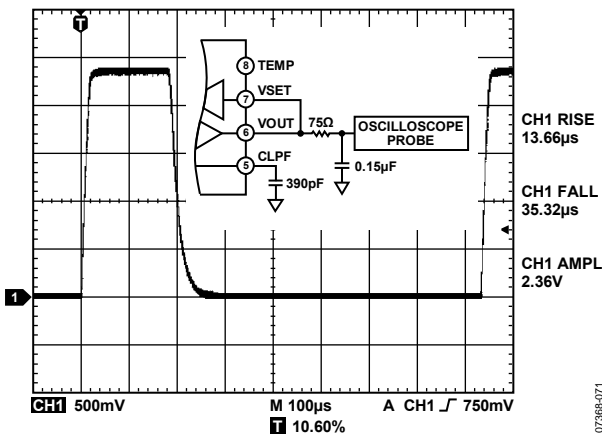


Figure 52. Pulse Response with  $C_{LPF} = 390$  pF and Series 75  $\Omega$  Resistor Followed by a 0.15  $\mu$ F Capacitor to Ground, Resulting in a 150 mV p-p Ripple for a Single Carrier CDMA2000 9CH SR1 Signal at 2.14 GHz

### RF PULSE RESPONSE AND VTGT

The response of the AD8363 to pulsed RF waveforms is affected by  $V_{TGT}$ . Referring to Figure 21 and Figure 22, there is a period of inactivity between the start of the RF waveform and the time at which  $V_{OUT}$  begins to show a reaction. This happens as a result of the implementation of the balancing of the squarer currents within the AD8363. This delay can be reduced by decreasing  $V_{TGT}$ ; however, as previously noted in the VTGT Interface section, this has implications on the sensitivity, intercept, and dynamic range. While the delay is reduced, reducing  $V_{TGT}$  increases the rise and fall time of  $V_{OUT}$ .

### CONTROLLER MODE BASIC CONNECTIONS

In addition to being a measurement device, the AD8363 can also be configured to control rms signal levels, as shown in Figure 53.

The RF input to the device is configured as it was in measurement mode and either input can be used. A directional coupler taps off some of the power being generated by the VGA. If loss in the main signal path is not a concern, and there are no issues with reflected energy from the next stage in the signal chain, a power splitter can be used instead of a directional coupler. Some additional attenuation may be required to set the maximum input signal at the AD8363 to be equal to the recommended maximum input level for optimum linearity and temperature stability at the frequency of operation.

The VSET and VOUT pins are no longer shorted together. VOUT now provides a bias or gain control voltage to the VGA. The gain control sense of the VGA must be negative and monotonic, that is, increasing voltage tends to decrease gain. However, the gain control transfer function of the device does not need to be well controlled or particularly linear. If the gain control sense of the VGA is positive, an inverting op amp circuit with a dc offset shift can be used between the AD8363 and the VGA to keep the gain control voltage in the 0.03 V to 4.8 V range.

VSET becomes the set-point input to the system. This can be driven by a DAC, as shown in Figure 53, if the output power is expected to vary, or it can simply be driven by a stable reference voltage, if constant output power is required. This DAC should have an output swing that covers the 0.15 V to 3.5 V range.

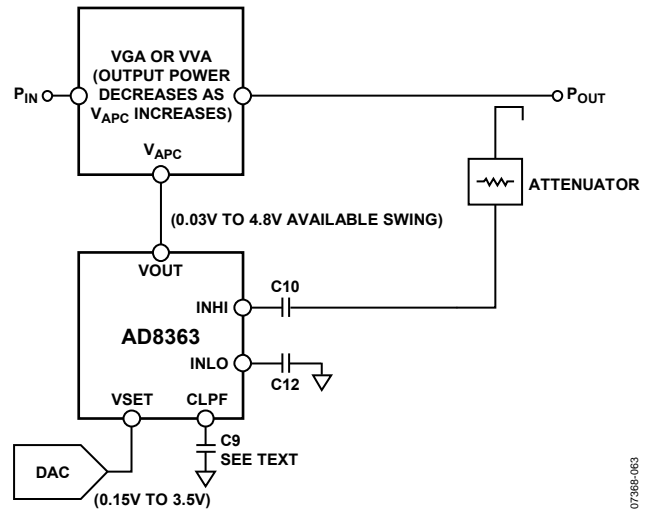


Figure 53. Controller Mode Operation for Automatic Power Control

When  $V_{SET}$  is set to a particular value, the AD8363 compares this value to the equivalent input power present at the RF input. If these two values do not match,  $V_{OUT}$  increases or decreases in an effort to balance the system. The dominant pole of the error amplifier/integrator circuit that drives  $V_{OUT}$  is set by the capacitance on the CLPF pin; some experimentation may be necessary to choose the right value for this capacitor.

In general,  $C_{LPF}$  should be chosen to provide stable loop operation for the complete output power control range. If the slope (in dB/V) of the gain control transfer function of the VGA is not constant,  $C_{LPF}$  must be chosen to guarantee a stable loop when the gain control slope is at its maximum. In addition,  $C_{LPF}$  must provide adequate averaging to the internal low range squaring detector so that the rms computation is valid. Larger values of  $C_{LPF}$  tend to make the loop less responsive.

The relationship between  $V_{SET}$  and the RF input follows the measurement mode behavior of the device. For example, Figure 4 shows the measurement mode transfer function at 900 MHz and that an input power of  $-10$  dBm yields an output voltage of approximately 2.5 V. Therefore, in controller mode, if  $V_{SET}$  is 2.5 V, the AD8363 output would go to whatever voltage is necessary to set the AD8363 input power to  $-10$  dBm.

**CONSTANT OUTPUT POWER OPERATION**

In controller mode, the AD8363 can be used to hold the output power of a VGA stable over a broad temperature/input power range. This is useful in topologies where a transmit card is driving an HPA, or when connecting any two power sensitive modules together.

Figure 54 shows a schematic of a circuit setup that holds the output power to approximately  $-26$  dBm at 2.14 GHz, when the input power is varied over a 40 dB dynamic range. Figure 55 shows the results. A portion of the output power is coupled off using a 10 dB directional coupler, and it is then fed into the AD8363.  $V_{SET}$  is fixed at 0.95 V, which forces the AD8363 output voltage to control the ADL5330 so that the input to the AD8363 is approximately  $-36$  dBm.

If the AD8363 was in measurement mode and a  $-36$  dBm input power is applied, the output voltage would be 0.95 V. A general-purpose, rail-to-rail op amp (AD8062) is used to invert the slope of the AD8363 so that the gain of the ADL5330 decreases as the AD8363 control voltage increases. The output power is controlled to a 10 dB higher power level than that seen by the AD8363 due to the coupler. The high-end power is limited by the linearity of the VGA (ADL5330) with high attenuation and can be increased by using a higher linearity VGA.

The low end power is limited by the maximum gain of the VGA (ADL5330) and can be increased by using a VGA with more gain. The temperature performance is directly related to the temperature performance of the AD8363 at 2.14 GHz and  $-26$  dBm, using  $TCM1 = 0.52$  V and  $TCM2 = 0.6$  V. All other temperature variations are removed by the AD8363.

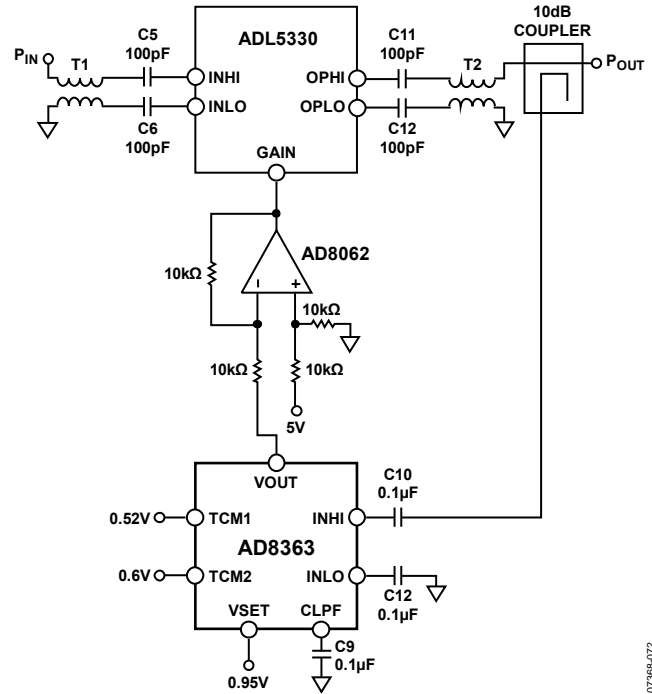


Figure 54. Constant Power Circuit

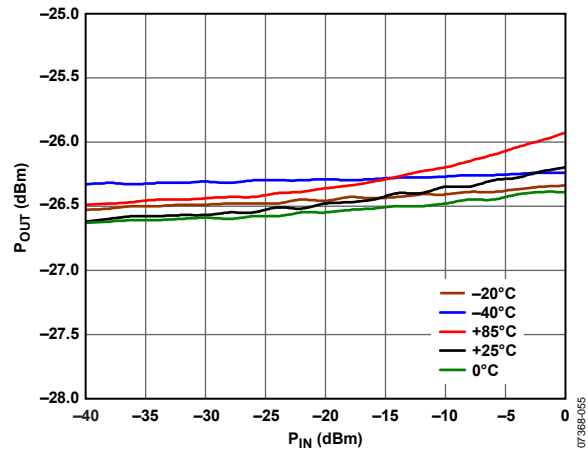


Figure 55. Performance of the Circuit Shown in Figure 54



**DESCRIPTION OF RF CHARACTERIZATION**

The general hardware configuration used for most of the AD8363 characterization is shown in Figure 56. The AD8363 was driven in a single-ended configuration for all characterization.

Characterization of the AD8363 employed a multisite test strategy. Several AD8363 devices mounted on circuit boards constructed with Rogers 3006 material was simultaneously inserted into a remotely-controlled thermal test chamber. A Keithley S46 RF switching network connected an Agilent E8251A signal source to the appropriate device under test. An Agilent 34980A switch matrix provided switching of dc power and metering for the test sites. A PC running Agilent VEE Pro controlled the signal source, switching, and chamber temperature.

A voltmeter measured the subsequent response to the stimulus, and the results were stored in a database for later analysis. In this way, multiple AD8363 devices were characterized over amplitude, frequency, and temperature in a minimum amount of time.

The RF stimulus amplitude was calibrated up to the connector of the circuit board that carries the AD8363. However, the calibration does not account for the slight losses due to the connector and the traces from the connector to the device under test. For this reason, there is a small absolute amplitude error (<0.5 dB) not accounted for in the characterization data.

This implies a slight error in the reported intercept; however, this is generally not important because the slope and the relative accuracy of the AD8363 are not affected.

The typical performance data was derived with  $C_{LPF} = 3.9 \text{ nF}$  and  $C_{HPF} = 2.7 \text{ nF}$  with a CW waveform.

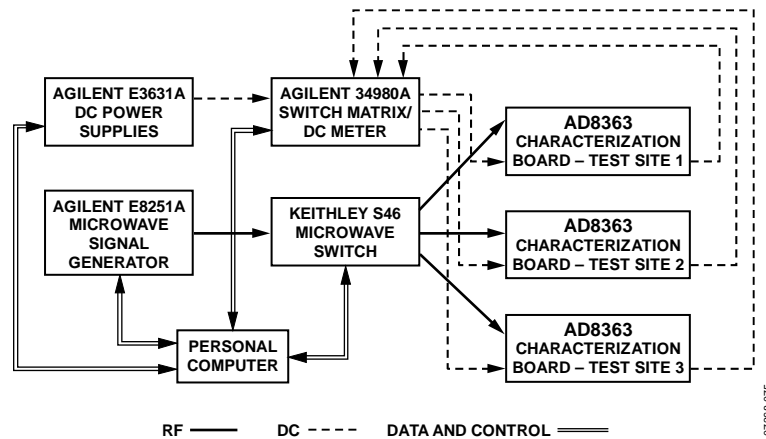


Figure 56. General RF Characterization Configuration

**EVALUATION AND CHARACTERIZATION CIRCUIT BOARD LAYOUTS**

Figure 57 to Figure 61 show the evaluation board for the [AD8363](#).

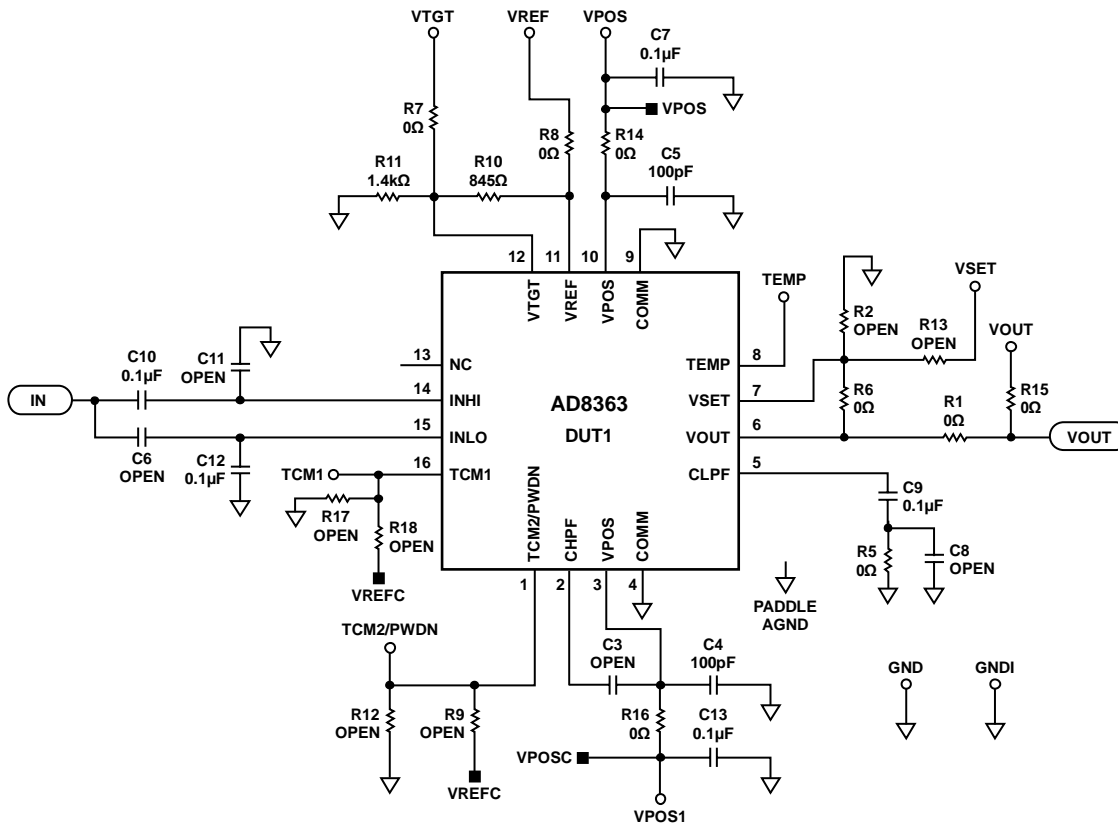


Figure 57. Evaluation Board Schematic

072889-074

Table 6. Evaluation Board Configuration Options

Component	Function/Notes	Default Value
C6, C10, C11, C12	Input. The AD8363 is single-ended driven. At frequencies $\leq 2.6$ GHz, the best dynamic range is achieved by driving Pin 14 (INHI). When driving INHI, populate C10 and C12 with an appropriate capacitor value for the frequency of operation and leave C6 and C11 open. For frequencies $> 2.6$ GHz, additional dynamic range can be achieved by driving Pin 15 (INLO). When driving INLO, populate C6 and C11 with an appropriate capacitor value for the frequency of operation and leave C10 and C12 open.	C6 = open, C10 = 0.1 $\mu$ F, C11 = open C12 = 0.1 $\mu$ F
R7, R8, R10, R11	VTGT. R10 and R11 are set up to provide 1.4 V to VTGT from VREF. If R10 and R11 are removed, an external voltage can be used. Alternatively, R7 and R11 can be used to form a voltage divider for an external reference.	R7 = 0 $\Omega$ , R8 = 0 $\Omega$ , R10 = 845 $\Omega$ , R11 = 1.4 k $\Omega$
C4, C5, C7, C13, R14, R16	Power Supply Decoupling. The nominal supply decoupling consists of a 100 pF filter capacitor placed physically close to the AD8363, a 0 $\Omega$ series resistor, and a 0.1 $\mu$ F capacitor placed close to the power supply input pin. The 0 $\Omega$ resistor can be replaced with a larger resistor to add more filtering; however, it is at the expense of a voltage drop.	C4 = 100 pF, C5 = 100 pF, C7 = 0.1 $\mu$ F, C13 = 0.1 $\mu$ F, R14 = 0 $\Omega$ , R16 = 0 $\Omega$
R1, R2, R6, R13, R15	Output Interface (Default Configuration) in Measurement Mode. In this mode, a portion of the output voltage is fed back to the VSET pin via R6. Using the voltage divider created by R2 and R6, the magnitude of the slope at VOUT is increased by reducing the portion of VOUT that is fed back to VSET. If a fast responding output is expected, the 0 $\Omega$ resistor (R15) can be removed to reduce parasitics on the output.  Output Interface in Controller Mode. In this mode, R6 must be open and R13 must have a 0 $\Omega$ resistor. In controller mode, the AD8363 can control the gain of an external component. A setpoint voltage is applied to the VSET pin, the value of which corresponds to the desired RF input signal level applied to the AD8363. If a fast responding output is expected, the 0 $\Omega$ resistor (R15) can be removed to reduce parasitics on the output.	R1 = 0 $\Omega$ , R2 = open, R6 = 0 $\Omega$ , R13 = open, R15 = 0 $\Omega$
C8, C9, R5	Low-Pass Filter Capacitors, $C_{LPF}$ . The low-pass filter capacitors reduce the noise on the output and affect the pulse response time of the AD8363. This capacitor should be as large as possible. The smallest $C_{LPF}$ capacitance should be 390 pF. R5, when set to a value other than 0 $\Omega$ , is used in conjunction with C8 and C9 to modify the loop transfer function and change the loop dynamics in controller mode.	C8 = open, C9 = 0.1 $\mu$ F, R5 = 0 $\Omega$
C3	$C_{HPF}$ Capacitor. The $C_{HPF}$ capacitor introduces a high-pass filter affect into the AD8363 transfer function and can also affect the response time. The $C_{HPF}$ capacitor should be as small as possible and connect to VPOS when used. No capacitor is needed for input frequencies greater than 10 MHz.	C3 = open
R9, R12	TCM2/PWDN. The TCM2/PWDN pin controls the amount of nonlinear intercept temperature compensation and/or shuts down the device. The evaluation board is configured to control this from a test loop, but VREF can also be used by the voltage divider created by R9 and R12.	R9 = open, R12 = open
R17, R18	TCM1. TCM1 controls the temperature compensation (5 k $\Omega$ impedance). The evaluation board is configured to control this from a test loop, but VREF can also be used by the voltage divider created by R17 and R18. Due to the relatively low impedance of the TCM1 pin and the limited current of the VREF pin, care should be taken when choosing the R17 and R18 values.	R17 = open, R18 = open
Paddle	Connect the paddle to both a thermal and electrical ground.	

ASSEMBLY DRAWINGS

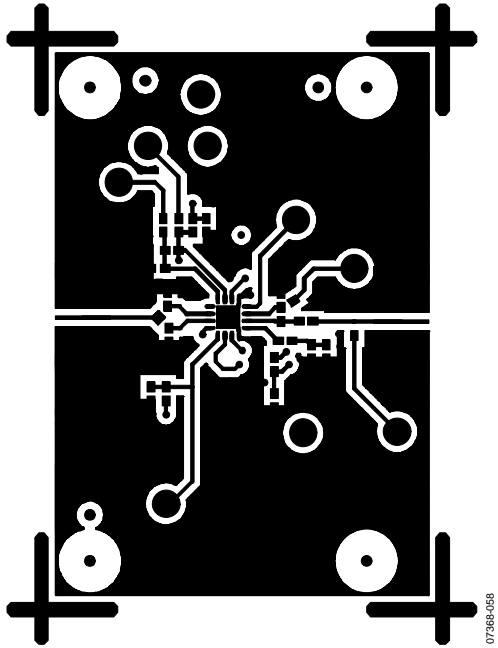


Figure 58. Evaluation Board Layout, Top Side

07363-060

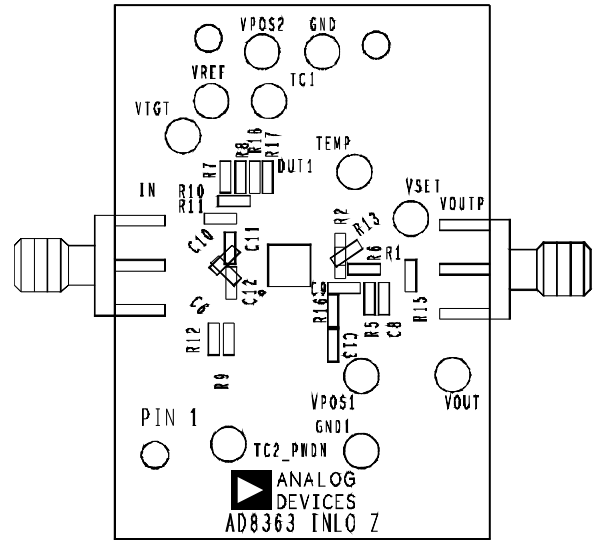


Figure 60. Evaluation Board Assembly, Top Side

07363-060

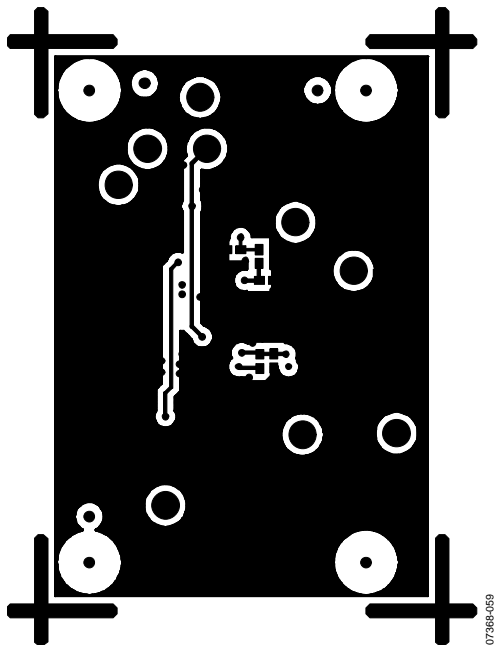


Figure 59. Evaluation Board Layout, Bottom Side

07363-060

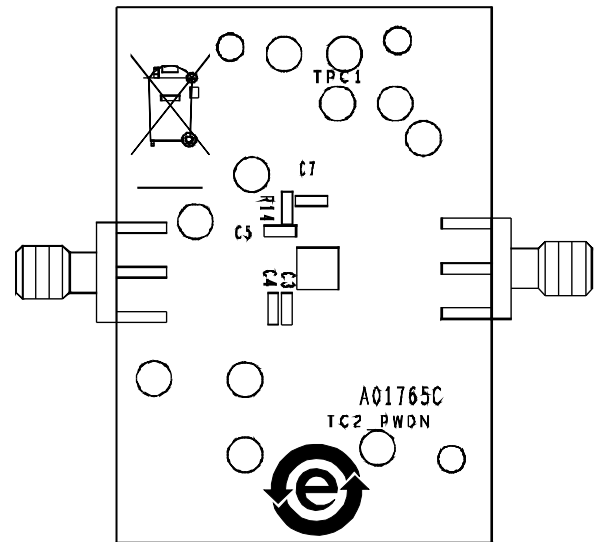
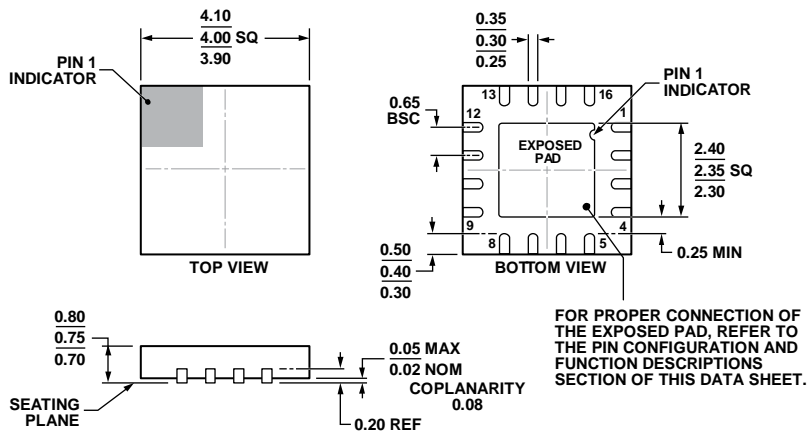


Figure 61. Evaluation Board Assembly, Bottom Side

07363-061

# OUTLINE DIMENSIONS



COMPLIANT TO JEDEC STANDARDS MO-220-WGGC-3.

Figure 62. 16-Lead Lead Frame Chip Scale Package [LFCSP\_WQ]  
 4 mm × 4 mm Body, Very Very Thin Quad  
 (CP-16-20)  
 Dimensions shown in millimeters

07-18-2012-B

## ORDERING GUIDE

Model <sup>1</sup>	Temperature Range	Package Description	Package Option	Ordering Quantity
AD8363ACPZ-R2	-40°C to +125°C	16-Lead Lead Frame Chip Scale Package [LFCSP_WQ]	CP-16-20	250
AD8363ACPZ-R7	-40°C to +125°C	16-Lead Lead Frame Chip Scale Package [LFCSP_WQ]	CP-16-20	1,500
AD8363ACPZ-WP	-40°C to +125°C	16-Lead Lead Frame Chip Scale Package [LFCSP_WQ]	CP-16-20	64
AD8363-EVALZ		Evaluation Board		

<sup>1</sup> Z = RoHS Compliant Part.

## X-ON Electronics

Largest Supplier of Electrical and Electronic Components

*Click to view similar products for [RF Detector](#) category:*

*Click to view products by [Analog Devices](#) manufacturer:*

Other Similar products are found below :

[HMC439QS16GTR](#) [HMC7447-SX](#) [MACP-010562-TR1000](#) [R451075000](#) [2085-6013-13](#) [2085-6010-00](#) [32-2018-BU](#) [32-3033-BU](#) [32-3203-BU](#) [AD8361ARMZ-REEL](#) [LT5534ESC6#TRPBF](#) [AD8361ARM-REEL7](#) [AD8314ARMZ-REEL](#) [AD8311ACBZ-P7](#) [AD8312ACBZ-P7](#) [AD8313ARMZ-REEL7](#) [AD8314ACPZ-RL7](#) [AD8314ARMZ](#) [AD8314ARMZ-REEL7](#) [AD8315ARMZ](#) [AD8317ACPZ-R7](#) [AD8319ACPZ-R7](#) [AD8361ARMZ](#) [AD8361ARMZ-REEL7](#) [AD8362ARUZ-REEL7](#) [AD8363ACPZ-R7](#) [AD8302ARUZ-RL7](#) [ADL5906ACPZN-R7](#) [ADL5500ACBZ-P7](#) [ADL5502ACBZ-P7](#) [ADL5504ACBZ-P7](#) [ADL5505ACBZ-P7](#) [ADL5506ACBZ-R7](#) [ADL5506WACBZ-R7](#) [ADL5513ACPZ-R7](#) [ADL5903ACPZN-R7](#) [ADL5903SCPZN-R7](#) [ADL6010ACPZN-R2](#) [ADL6010SCPZN](#) [ADL6010SCPZN-R7](#) [ADL6010SCPZN-R2](#) [ADL6012ACPZN](#) [ADL5511ACPZ-R7](#) [ADL5904ACPZN-R7](#) [ADL5910ACPZN-R7](#) [AD8364ACPZ-REEL7](#) [ADL5920ACPZ](#) [HMC1021LP4E](#) [HMC1120LP4E](#) [HMC1120LP4ETR](#)